




Article

Shrubs Matter: An Evaluation of the Capacity of Nine Shrub Species to Dissipate Latent Heat and to Remove CO₂ and Airborne PM

Sebastien Comin^{1,2,*}, Denise Corsini¹, Irene Vigevani^{3,4}, Caterina Villa⁵, Christian Bettosini⁶, Elena Crescini⁷, Paolo Viskanic⁸, Francesco Ferrini^{4,9} and Alessio Fini¹

¹ Department of Agricultural and Environmental Sciences—Production, Landscape, Agroenergy, University of Milan, 20133 Milan, Italy; denise.corsini@unimi.it (D.C.); alessio.fini@unimi.it (A.F.)

² Department of Earth and Environmental Science, University of Milan Bicocca, 20126 Milan, Italy

³ Department of Sciences, Technologies and Society, University School for Advanced Studies IUSS Pavia, 27100 Pavia, Italy; irene.vigevani@iusspavia.it

⁴ Department of Agriculture, Food, Environment and Forestry, University of Florence, 50144 Florence, Italy; francesco.ferrini@unifi.it

⁵ Demetra, 20842 Besana Brianza, Italy; denva@demetra.net

⁶ Public Green Service, Urban Space Division, 6900 Lugano, Switzerland; christian.bettosini@lugano.ch

⁷ Municipal Green Service, 39030 Bolzano, Italy; elena.crescini@comune.bolzano.it

⁸ R3 GIS S.r.l., NOI Techpark, 39100 Bolzano, Italy; paolo.viskanic@r3gis.com

⁹ Laboratory for Value, Joint Lab University of Florence—Italian Society for Horticultural Science (SOI), 50019 Sesto Fiorentino, Italy

* Correspondence: sebastien.comin@unimi.it

Abstract

The aim of this research was to quantify the capacity of different shrub species to remove atmospheric CO₂, to adsorb particulate matter and to dissipate latent heat through transpiration. A total of 308 established plants comprising *Deutzia scabra*, *Elaeagnus × ebbingei*, *Euonymus japonicus*, *Forsythia × intermedia*, *Laurus nobilis*, *Ligustrum vulgare*, *Pittosporum tobira*, *Prunus laurocerasus* and *Viburnum tinus* were selected in Lugano (Switzerland) and Bolzano (Italy). Stem diameter, crown radius, Leaf Area Index, net CO₂ assimilation per unit leaf area (A_{leaf}), transpiration, and stomatal conductance (g_s) were measured during spring, summer, and fall. The net CO₂ assimilation per unit of crown projection area and per plant were calculated by upscaling A_{leaf} using a multilayer model. Latent heat dissipation was calculated using the Penman–Monteith equation. The amount of PM trapped on leaves was measured using a gravimetric method. Differences in leaf area and leaf gas exchange among species affected their capacity to deliver specific ecosystem services. *Forsythia*, *Pittosporum*, *Elaeagnus* and *Deutzia* removed about 40% more CO₂ per unit crown projection area than *Laurus*, *Ligustrum*, and *Euonymus*. Latent heat dissipation by shrubs was, on average, 130 W m⁻², which is comparable to that of tree species. PM removal per unit leaf area was higher in species with sparse canopies and rough leaf surfaces.

Keywords: allometric equations; CO₂ assimilation; latent heat; Leaf Area Index; particulate matter; ecosystem services



Academic Editors: Milos Davidovic and Saverio De Vito

Received: 23 February 2026

Revised: 27 April 2026

Accepted: 29 April 2026

Published: 20 May 2026

Copyright: © 2026 by the authors.

Licensee MDPI, Basel, Switzerland.

This article is an open access article distributed under the terms and conditions of the [Creative Commons Attribution \(CC BY\) license](https://creativecommons.org/licenses/by/4.0/).

1. Introduction

Urban vegetation can contribute to the well-being of city dwellers through the delivery of provisioning, environmental regulation and support, and cultural ecosystem services [1]. A growing body of research focuses on methods and parameters to quantify the delivery

of ecosystem services (ES) by urban vegetation species [2–5]; however, most studies deal with tree species. While data about shrubs are rarer [6], the value of shrubs should not be underestimated. Unlike trees, they can be planted in very small spaces, along road edges where they do not pose any risk of interference with vehicular traffic, nor risk causing negative impact on air quality, which happens for large trees in urban street canyons [7]. Shrubs are known to effectively contribute to the removal of atmospheric particulate matter. According to the *Lancet* report for 2025, deaths attributable to total ambient PM_{2.5} air pollution increased from 7.5 million deaths in 2010 to 8.5 million deaths in 2022 (7.6% increase); while deaths attributable to ambient PM_{2.5} air pollution from human activities grew from 5.9 million in 2010 to 6.5 million in 2022 (11.3% increase) [8].

The effectiveness of shrubs to reduce atmospheric CO₂, estimated as carbon storage (C-storage) (i.e., the amount of atmospheric carbon trapped as organic carbon in the woody biomass of the tree) or C-sequestration (i.e., the change in carbon storage over 1 year) [9], is generally reported as low, because of their smaller size and biomass at maturity compared to trees [10]. Nonetheless, the contribution of vegetation to CO₂ removal may be better represented by net photosynthetic carbon gain (i.e., the amount of atmospheric CO₂ annually removed by vegetation through photosynthesis, net of respiratory losses) [4]. Shrubs can develop high Leaf Area Index (LAI) and can have high photosynthetic rate per unit leaf area, thus their role in CO₂ removal may be higher than previously thought [6]. Direct measurements of CO₂ assimilation have seldom been conducted in situ at urban sites, and in most cases, they were performed only on full-sun leaves [11]. Conversely, the parametrization of shaded leaves is crucial to upscale photosynthesis from leaf-scale to canopy-scale using sun–shade models, which were shown to be more accurate than big-leaf models [12].

Similarly, most of the research that evaluated the capacity of urban vegetation to ameliorate microclimate mostly focused on trees [13–15]. Due to larger canopy size and total leaf area, trees are expected to shade (i.e., reduce the amount of short-wave radiation reaching surfaces and buildings, and consequently, heat accumulation) and to dissipate latent heat through transpiration more efficiently than shrubs [16]. Nonetheless, the shrub layer can positively contribute to urban canopy cover, which is a major determinant of cooling benefits [17], and the use of shrub species that sustain a high stomatal conductance during hot periods may help the city to become more climate-proof.

Finally, the effect of shrubs on air particulate matter (PM) reduction, especially when forming ‘vegetation barriers’ or ‘green belts’ along roads, was studied in situ in a limited number of species [18–20]. Vegetation can passively ameliorate air quality through two main mechanisms: deposition and dispersion. Pollutant particles can be deposited on plant surfaces (i.e., bark and leaves) by rain and snow or by gravity, inertia and Brownian motion (deposition mechanism). At the same time, plants can alter air currents and turbulence simply through their physical presence, influencing the local concentration of pollutants (dispersion mechanism) [21]. The value of shrubs compared to trees in this field is particularly relevant. Shrub-specific traits, such as the canopy structure (often multi-stemmed and branched from the ground) and the limited height, allow for the creation of thick and dense green barriers very close to vehicular emission sources of air PM, efficiently reducing pedestrian exposure to air pollution in open road conditions [7]. Even in urban street canyons, shrubs are more effective than large trees. The latter of the two, even when able to trap many particles, still does not prevent the flow of air pollutants at the pedestrian level because their crowns are generally above the average human breathing height of 1.5 m [7]. For all these reasons, more attention should be paid to the evaluation of the capacity of shrub species to ameliorate air quality. Despite the relevance of these processes, relatively few studies have specifically quantified the ecosystem services provided by

shrubs in urban environments, and the available literature on shrub-derived benefits remains limited.

This research used two cities (Lugano, Switzerland; Bolzano, Italy) as living laboratories to test in situ the hypothesis that the capacity to assimilate CO₂, dissipate latent heat through transpiration, and remove atmospheric PM differs among shrub species due to differences in physiological traits and leaf area. Additionally, we tested the idea that ES provisioning may vary across different seasons depending on the meteorological variables of the planting site. These findings will provide useful support for decision makers during the selection of shrub species for urban planting in order to maximize plant and human wellbeing.

2. Materials and Methods

2.1. Experimental Sites and Plant Material

The research was carried out in Lugano (Switzerland) and Bolzano (Italy). Both cities have a temperate, mild and humid climate (Cfb, according to the Koppen–Geiger classification). The average air temperature over the last 30 years is 14.0 °C in Lugano and 13.1 °C in Bolzano. January is the coldest month in both cities (average temperatures are 3.8 °C and 1.8 °C in Lugano and Bolzano, respectively), and July is the warmest month, with an average temperature of 22.6 °C in Lugano and 23.7 °C in Bolzano. Rainfall is evenly distributed throughout the year in both cities, and the average annual rainfall is substantially higher in Lugano (1658 mm per year) than in Bolzano (1111 mm per year). Over the experimental period (January 2020 to December 2020 for Lugano and January 2021 to December 2021 for Bolzano), daily weather data were obtained from the local weather stations of the two cities (MeteoSwiss for Lugano, Open data Alto Adige for Bolzano), while daily air pollutant data were obtained from local stations (OASI—Osservatorio Ambientale della Svizzera Italiana for Lugano, Agenzia provinciale per l’ambiente e la tutela del clima for Bolzano) (Table 1).

Table 1. Meteorological and air quality data from the experimental sites of Lugano (a) and Bolzano (b) across a 16–17-day period (pre-sampling period of 14 days plus 2–3 sampling days).

City	Sampling Period	Season	Precipitation, Cumulative Values (mm)	Wind Velocity (m s ⁻¹)	PM _{2.5} Concentration (µg m ⁻³)	PM ₁₀ Concentration (µg m ⁻³)
(a) Lugano	16 to 18 June 2020	spring	294.0	1.47	4.21	8.25
	27–28 July 2020	summer	25.5	1.54	7.69	13.68
	16–17 September 2020	fall	16.8	1.23	11.47	18.67
	12 to 14 January 2021	winter	50.3	1.28	14.55	19.94
(b) Bolzano	26–27 May 2021	spring	38.2	1.58	4.26	7.62
	20–21 July 2021	summer	64.6	1.56	7.52	12.51
	30 September to 1 October 2021	fall	47.3	1.07	8.83	13.91
	26–27 January 2021	winter	32.7	1.19	15.51	23.94

During the experimental years (2020 and 2021), the annual average air PM₁₀ and PM_{2.5} concentrations obtained from the local stations were 18.5 and 12.3 µg m⁻³, respectively, in Lugano, and 17.2 and 11 µg m⁻³ in Bolzano. In both cases, the values were above the WHO guideline recommendations (annual averages of PM₁₀ < 15 µg m⁻³ and PM_{2.5} < 5 µg m⁻³; [22]), and PM_{2.5} also exceeded the new thresholds recently proposed for Europe (annual averages of PM₁₀ < 20 µg m⁻³ and PM_{2.5} < 10 µg m⁻³) [22]. Weather and average daily air PM₁₀ and PM_{2.5} concentrations are reported for the different measurement days in Tables 1 and 2. During the sampling days, air PM₁₀ concentration never exceeded the WHO recommendations (PM₁₀ < 45 µg m⁻³; 24-h average) while air PM_{2.5}

concentrations slightly exceeded the WHO recommendations ($PM_{2.5} < 15 \mu\text{g m}^{-3}$; 24-h average) in Bolzano during winter.

Table 2. Average temperature and cumulative precipitation in the experimental site of Lugano (a) and Bolzano (b) compared to the average values of the last thirty years: spring (01/05 to 21/06), summer (22/06 to 31/08), fall (01/09 to 15/10) and winter (01/01 to 29/02).

City	Year	Season	Precipitation, Cumulative Values (mm)	Precipitation, Avg Last Thirty Years (mm)	Temperature (°C)	Temperature, Avg Last Thirty Years (°C)
(a) Lugano	2020	spring	510	164	19.7	19.6
		summer	50	153	23.1	22.1
		fall	130	185	18.9	17.5
		winter	175	127	5.2	4.4
(b) Bolzano	2021	spring	98	70	17.3	18.0
		summer	133	87	24.4	24.7
		fall	47	70	21.1	18.5
		winter	180	52	2.3	1.5

Six shrub species per city were selected based on their relevance in the existing plant inventories and their even distribution in the cities. The list of species, their abbreviations, the number of plants on which growth traits were assessed, and their minimum and maximum stem diameters and crown projection area are reported in Table 3. Three of the six species [the deciduous *Forsythia × intermedia* (Fi), the evergreen *Pittosporum tobira* (Pt) and *Prunus laurocerasus* (Pl)] were measured in both cities. The evergreen *Elaeagnus × ebbingei* (Ee) and *Laurus nobilis* (Ln) and the semi-deciduous *Ligustrum vulgare* (Lv) were only measured in Lugano. The deciduous *Deutzia scabra* (Ds) and the evergreen *Euonymus japonicus* (Ej) and *Viburnum tinus* (Vt) were only sampled in Bolzano. To representatively sample the shrub population, the location of the selected shrub species growing in each city was retrieved using the existing city inventory implemented into GREENSPACES software (R3GIS, Bolzano, Italy). Nine (Lugano) and eight (Bolzano) blocks containing at least 2 individuals of every selected species were established in each city. The blocks were evenly distributed and included public parks, school gardens, and roadside vegetation (Figure A1 in Appendix A). Shrubs growing solitary or in shrubby patches were preferred over those growing in formal hedges.

Table 3. Species selected in the experimental cities of Lugano (a) and Bolzano (b), their abbreviations, and the number of plants on which biometrics parameters were measured. D_{30min} (cm), D_{30max} (cm) and CPA_{min} (m²), CPA_{max} (m²) indicate the observed minimum and maximum stem diameters and crown projection areas, respectively. H_{avg} (m) indicates the average plant height recorded. Standard deviation is reported for H_{avg} . E, D, SD in brackets in the species column indicate their leaf persistence: evergreen, deciduous and semi-deciduous, respectively. n is the number of analyzed shrubs per species.

City	Species	Abbreviation	n.	D_{30min} (cm)	D_{30max} (cm)	CPA_{min} (m ²)	CPA_{max} (m ²)	H_{avg} (m)
(a) Lugano	<i>Elaeagnus × ebbingei</i> (E)	Ee	23	4.47	18.60	0.86	20.39	2.01 ± 0.7
	<i>Forsythia × intermedia</i> (D)	Fi	24	3.85	15.34	1.43	19.15	3.13 ± 1
	<i>Laurus nobilis</i> (E)	Ln	22	4.02	42.70	0.23	16.38	2.97 ± 2.4
	<i>Ligustrum vulgare</i> (SD)	Lv	23	3.17	12.00	0.35	8.79	1.91 ± 0.4
	<i>Pittosporum tobira</i> (E)	Pt	24	3.39	36.47	1.09	35.45	2.20 ± 1.5
	<i>Prunus laurocerasus</i> (E)	Pl	24	7.49	27.80	0.43	9.84	2.44 ± 0.7
(b) Bolzano	<i>Deutzia scabra</i> (D)	Ds	30	2.48	17.70	0.28	15.16	2.20 ± 0.9
	<i>Euonymus japonicus</i> (E)	Ej	18	2.74	22.98	0.50	32.12	2.10 ± 1.2
	<i>Forsythia × intermedia</i> (D)	Fi	30	2.14	11.78	0.49	10.70	2.23 ± 0.9
	<i>Pittosporum tobira</i> (E)	Pt	30	6.70	25.43	0.78	35.44	2.44 ± 0.9
	<i>Prunus laurocerasus</i> (E)	Pl	30	2.37	31.86	0.64	77.70	2.22 ± 1.2
	<i>Viburnum tinus</i> (E)	Vt	30	2.33	14.48	0.33	6.67	2.02 ± 0.6

2.2. Growth and Leaf Area Index

Biometric measurements were performed in January 2021 on all individuals of the selected species growing in the experimental areas (140 and 158 plants in Lugano and Bolzano, respectively). The number of stems and their diameter, crown radius and plant height were recorded. Stem diameters (D_{30}) were measured at 30 cm from the ground [23] with a caliper, by making two measurements perpendicular to each other and averaging the measured values. For shrubs with less than six stems, all the diameters were measured, then the radius ($r = d/2$) and the corresponding basal stem area ($A = \pi r^2$) were calculated. The areas of the individual stems were summed (A_{tot}), then the overall stem radius (r_{tot}) and diameter (D_{tot}) were calculated as: $r_{tot} = \sqrt{A_{tot}/\pi}$; $D_{tot} = 2 \times r_{tot}$. For shrubs with more than six stems, six representative stems were chosen and their diameters measured. The average basal area of the 6 stems was calculated, then multiplied by the number of stems to get A_{tot} . r_{tot} and D_{tot} were calculated as described previously. Crown projection area (CPA) was calculated from two orthogonal crown diameter measurements, performed using a mm accuracy diameter tape in the North–South and East–West direction as: $CPA = \pi \times (d_{NS}/2 \times d_{EW}/2)$. Plant height was measured using a cm accuracy diameter tape.

The effective Plant Area Index (PAI_e , $m^2 m^{-2}$) was measured using an Accupar ceptometer (Accupar LP-80, Decagon Devices, Washington, DC, USA) during bright days ($PAR > 1300 \mu mol m^{-2} s^{-1}$ and progressive change in $PAR < 75 \mu mol m^{-2} min^{-1}$) in July 2020 and July 2021. Measurements were carried out between 11:30 and 14:30 (CET) [24], on the same shrubs subjected to the eco-physiological measurements. Four readings of above-canopy irradiance (measured by positioning the ceptometer horizontally above the canopy) and below-canopy irradiance were collected per plant [25]. To account for Woody Area Index (WAI , $m^2 m^{-2}$), a WAI/PAI ratio (α) of 0.25 was assumed based on available literature on shrubs [26–28]. To account for the non-normal leaf distribution within the canopy, clumping (Ω) was calculated as described by [29], assuming a uniform vertical profile of PAI_e . Leaf Area Index (LAI , $m^2 m^{-2}$), i.e., half of total leaf surface area per unit ground surface area, was calculated as:

$$LAI = (1 - \alpha) \times PAI_e / \Omega \quad (1)$$

2.3. Eco-Physiological Measurements

2.3.1. Net CO₂ Assimilation

Net CO₂ assimilation per unit leaf area (A_{leaf} , $\mu mol m^{-2} s^{-1}$) was measured using an infra-red gas analyzer (Ciras-2, PP-System, Amesbury, MA, USA). Measurements were conducted during spring (Lugano: 16–18 June 2020; Bolzano: 26–27 May 2021), summer (Lugano: 27–28 July 2020; Bolzano: 20–21 July 2021) and fall (Lugano: 16–17 September 2020; Bolzano: 30 September–1 October 2021) between 9:00 and 17:00 (CET). Four fully expanded leaves per plant were measured (for a total of 648 and 576 leaves over the entire experiment in Lugano and Bolzano, respectively). Leaves were chosen after ideally dividing the canopy into two layers along its vertical profile: an apical (a) and a basal (b) layer, each representing 50% of the live canopy height. Within each layer, one external leaf fully exposed to solar irradiance (denoted as “ae” and “be” for apical and basal layers, respectively) and one internal leaf to the canopy subjected to self-shading (denoted as “ai” and “bi” for apical and basal layers, respectively) were analyzed. The IRGA was set to supply the leaves with a 400 ppm external CO₂ concentration, 70% of external RH, while the irradiance provided was different depending on the leaf position. External leaves (ae;

be) were exposed to saturating irradiance ($1300 \mu\text{mol m}^{-2} \text{s}^{-1}$), while internal leaves (ai; bi) were exposed to species-specific irradiance values, which were set as follows:

$$\text{PAR}_{\text{shade}} = \text{PAR}_{\text{sun}} \times \tau \quad (2)$$

where PAR_{sun} is the above-canopy PAR, while τ is the transmittance in the apical (τ_{ai}) and basal (τ_{bi}) layers of the canopy (Table A1 in Appendix A). τ_{ai} and τ_{bi} were obtained as the ratio between the PAR measured inside the canopy (in the apical and basal layer, respectively) and above the canopy [4]. $\text{PAR}_{\text{shade}}$ was in the range of 88–862 $\mu\text{mol m}^{-2} \text{s}^{-1}$ (ai leaves) and 50–495 $\mu\text{mol m}^{-2} \text{s}^{-1}$ (bi leaves), depending on species and solar zenith angle (θ).

According to the multilayer approach, the crown was divided into two layers, each made of sun and shaded leaves [29]. The LAI of each layer was partitioned between sun and shade using the equations:

$$\text{LAI}_{\text{sun}} = 2\cos\theta \times (1 - e^{-0.5 \times \Omega \times \text{LAI} / \cos\theta}) \quad (3)$$

$$\text{and } \text{LAI}_{\text{shade}} = \text{LAI} - \text{LAI}_{\text{sun}} \quad (4)$$

The net CO_2 assimilation per unit crown projection area (A_{cpa} , $\text{g m}^{-2} \text{ground h}^{-1}$) was calculated as (More information in Appendix A):

$$A_{\text{cpa}} = 0.5 \times (A_{\text{ae}} \times \text{LAI}_{\text{sun}} + A_{\text{ai}} \times \text{LAI}_{\text{shade}}) + 0.5 \times (A_{\text{be}} \times \text{LAI}_{\text{sun}} + A_{\text{bi}} \times \text{LAI}_{\text{shade}}) \quad (5)$$

The total net CO_2 assimilation per plant (A_{plant} , $\text{g plant}^{-1} \text{h}^{-1}$) was then calculated by multiplying A_{cpa} and CPA .

2.3.2. Stomatal Conductance and Latent Heat Dissipation

Daily latent heat dissipation by transpiration was calculated using a one-step Penman–Monteith approach. Transpiration per unit leaf area (E_{leaf} , $\text{mmol m}^{-2} \text{s}^{-1}$) and stomatal conductance to water vapor (g_s , $\text{mmol m}^{-2} \text{s}^{-1}$) were measured as previously described for A_{leaf} in Section 2.3.1. Nighttime measurements of g_s were also conducted between 23.00 and 01.00 (CET). The environmental variables needed to run the equation were obtained from the local weather stations of the two cities (MeteoSwiss for Lugano, Open data Alto Adige for Bolzano). The latent heat flux due to transpiration per soil square meter (LH_{cpa} ; W m^{-2}) was calculated on a daily scale, according to [30] (modified from [31]):

$$\text{LH}_{\text{cpa}} = \frac{\Delta Q + \rho_a C_p \frac{\text{VPD}}{R_a}}{\Delta + \gamma \left(1 + \frac{R_s}{R_a}\right)} \quad (6)$$

where Q is the available energy in W m^{-2} ; ρ_a is the mean air density at constant pressure (1.22 kg m^{-3}); C_p is the specific heat of air ($1.013 \text{ kJ kg}^{-1} \text{K}^{-1}$); Δ represents the slope of the saturation vapor pressure–temperature relationship; R_a is the aerodynamic resistance; and R_s is the surface resistance.

The contribution of each type of leaf (sun/shade) in each layer (apical/basal) to latent heat dissipation was calculated from independent measurements of g_s values conducted on ae, ai, be and bi leaves, both during the day and at night ($\text{LH}_{\text{cpa,day}}$ and $\text{LH}_{\text{cpa,night}}$). LH_{cpa} was then calculated as (more information in Appendix A):

$$\text{LH}_{\text{cpa}} = \text{LH}_{\text{cpa,day}} + \text{LH}_{\text{cpa,night}} \quad (7)$$

2.3.3. Air Particulate Matter Removal

Air particulate matter removal was assessed by in situ leaf sampling and subsequent ex situ laboratory analysis. Sampling was performed in spring (Lugano: 16–18 June 2020; Bolzano: 26–27 May 2021), summer (Lugano: 27–28 July 2020; Bolzano: 20–21 July 2021), fall (Lugano: 16–17 September 2020; Bolzano: 30 September–1 October 2021) and winter (Lugano: 12–14 January 2021; Bolzano: 26–27 January 2021) on the same shrubs selected for biometrics and eco-physiological traits. A leaf sample representative of the entire crown was collected from each shrub, resulting in 54 samples in Lugano and 48 in Bolzano for each of the spring, summer, and fall seasons. During winter, only evergreen and semi-deciduous species were sampled, for a total of 45 and 32 samples in Lugano and Bolzano, respectively. Thus, a total of 207 samples in Lugano and 176 samples in Bolzano were analyzed over the entire experiment. Samples were manually collected, immediately stored at $-20\text{ }^{\circ}\text{C}$ and analyzed within one week. Each sample, made of about $300\text{--}400\text{ cm}^2$ leaf area, was analyzed with a gravimetric technique described in detail in [32]. The number of leaves needed to cover the required sampled area depended on leaf size. To quantify PM_x accumulation per unit leaf area ($\mu\text{g cm}^{-2}$) (i.e., the amount of PM_x on the leaf surface at the time of sampling), each leaf sample was subjected to a washing procedure with 250 mL of deionized water for 60 s. The washing solution was then first filtered through a metal sieve (Fritsch analysensieb, Idar-Oberstein, Germany) to eliminate particles larger than $100\text{ }\mu\text{m}$ and sequentially filtered using 3 filters with increasing retention capacities (type 1288, retention: $10\text{ }\mu\text{m}$; type 391, retention: $2.5\text{ }\mu\text{m}$; and PTFE membrane, retention: $0.2\text{ }\mu\text{m}$) (Sartorius AG, Goettingen, Germany). Filtration was performed using a filtration apparatus equipped with a 47 mm glass filter funnel (Sartorius stedim, Sartorius AG, Goettingen, Germany) connected to an MV-50 vacuum pump (Comecta-Ivymen, Barcelona, Spain). Before filtration, the PTFE membranes were moistened with isopropyl alcohol to facilitate the process. Prior to filtration, each filter was dried at $60\text{ }^{\circ}\text{C}$ for 30 min in a drying chamber (WTB Binder 7200, Tuttlingen, Germany) and then left to stabilize (at 50% air relative humidity) for 120 min before being pre-weighed on a high-precision balance (ED224S-OCE, Sartorius, Germany). After filtration, filters were dried again, the weight was stabilized, and then post-weighed. To consider potential balance drifts, the tare was reweighed every 15 min. The amount of PM was determined by the difference between the post-weight and pre-weight. Three fractions of PM_x were collected during the entire filtration procedure: (1) large ($PM_{10\text{--}100}$), (2) coarse ($PM_{2.5\text{--}10}$) and (3) fine ($PM_{0.2\text{--}2.5}$). The PM_{10} fraction was obtained by adding the second to the third fraction, while the $PM_{2.5}$ fraction was considered equivalent to the third fraction. After filtration, the leaf area of each sample was measured using an A3 scanner (HP OfficeJet Pro 7740, HP Development Company, L.P., Palo Alto, CA, USA) and a leaf area software (Leaf Area Measurement, version 1.3, University of Sheffield A.P., Askew, UK). The PM_x accumulation was then expressed per unit leaf area ($\mu\text{g cm}^{-2}$).

To obtain PM deposition per unit leaf area ($\mu\text{g cm}^{-2}\text{ day}^{-1}$) (i.e., the change in accumulation over time), a linear trend of deposition over the accumulation measurements was assumed. Thus, deposition was calculated as accumulation divided by the number of days without rainfall since the last effective rain (i.e., the one assumed to wash off the particles from the leaves, considered here higher than 7 mm day^{-1}). Up to a maximum of 15 days from the effective rain was observed in this experiment. Thus, the amount of deposited PM_{10} ($depPM_{10}$) and $PM_{2.5}$ ($depPM_{2.5}$) was expressed per unit leaf area and time ($\mu\text{g cm}^{-2}\text{ day}^{-1}$). $depPM_x$ was upscaled to PM deposition per unit crown projection area ($depPM_{x,cpa}$, $\text{g m}^{-2}\text{ ground day}^{-1}$) as follows:

$$depPM_{x,cpa} = depPM_x \times LAI \times 10^{-2} \quad (8)$$

where 10^{-2} is the conversion factor from $\mu\text{g cm}^{-2}$ to g m^{-2} .

2.4. Statistics

All statistics were performed using SPSS software (IBM SPSS Statistics for Windows, Version 29.0 Armonk, NY, USA), while figures were drawn with SigmaPlot 12.5 (Systat Software Inc., San Jose, CA, USA). Data were analyzed using linear mixed models within each city, estimated using restricted maximum likelihood (REML), with denominator degrees of freedom for tests of fixed effects obtained via the Satterthwaite approximation. In the model “species”, “leaf position” and “season” were considered fixed factors, while “block” was considered a random factor. A homogeneous ante-dependence correlation structure (AD1) was chosen based on the best fitting. Leaf position was not considered when analyzing benefits expressed per unit crown projection area. Only the species factor was considered for Leaf Area Index ($LAI, \text{m}^{-2} \text{m}^{-2}$). The assumptions of normality and homoscedasticity were verified by visual inspection of the diagnostic plots. Homogeneous subsets were identified using Tukey’s and Sidak’s post hoc tests. The growth curves $DBH-R_{crown}$ and $DBH-H_{tot}$ were fitted using the curve fitting tool included in SPSS. Different functions (e.g., linear, power and logarithmic functions) were tested for fitting.

3. Results

3.1. Growth Curves

Leaf Area Index (LAI), stem diameter and crown radius of the different species were monitored in Lugano and Bolzano. LAI significantly differed among species both in Lugano ($p < 0.001$) and Bolzano ($p < 0.05$) (Table 4). In Lugano, *Ee*, *Ln*, *Pt* and *Pl* showed higher LAI than *Fi* and *Lv*. In Bolzano, LAI was similar among species except for *Pl*, which showed a higher LAI than *Ej* (Table 4). The three species that were monitored in both cities (*Fi*, *Pt* and *Pl*) exhibited, in general, higher LAI in Lugano than in Bolzano ($p < 0.05$).

Table 4. For each species and experimental site, Leaf Area Index ($LAI, \text{m}^2 \text{m}^{-2}$) values are shown, along with parameters (scaling constant (a) and exponent (b) and coefficient of determination (R^2) of the regression curves ($Y = a X^b$) describing the relationships between stem diameter at 30 cm height (D_{30}, m) and crown radius (R_{crown}, m), and between D_{30} and total plant height (H_{tot}, m). In the LAI column, different letters indicate significant differences among species.

Species	$LAI (\text{m}^2 \text{m}^{-2})$		$R_{crown} = a \times D_{30}^b$			$H_{tot} = a \times D_{30}^b$			
			a (m)	b	R^2	a (m)	b	R^2	
Lugano	<i>Elaeagnus × ebbingei</i>	5.60	a	4.182	0.604	0.375	6.839	0.573	0.579
	<i>Forsythia × intermedia</i>	3.73	b	8.335	0.455	0.139	8.335	0.455	0.139
	<i>Laurus nobilis</i>	4.20	ab	4.300	0.675	0.523	10.167	0.633	0.518
	<i>Ligustrum vulgare</i>	3.39	b	5.088	0.684	0.429	1.912	0.007	0.000
	<i>Pittosporum tobira</i>	4.63	ab	4.065	0.699	0.552	12.122	1.044	0.568
	<i>Prunus laurocerasus</i>	5.80	a	7.886	1.017	0.619	9.231	0.711	0.483
Bolzano	<i>Deutzia scabra</i>	3.38	ab	10.646	0.975	0.687	9.142	0.564	0.275
	<i>Euonymus japonicus</i>	3.07	b	10.270	0.955	0.938	7.519	0.561	0.802
	<i>Forsythia × intermedia</i>	3.54	ab	6.710	0.684	0.218	5.201	0.31	0.058
	<i>Pittosporum tobira</i>	3.83	ab	4.164	0.582	0.215	7.681	0.592	0.409
	<i>Prunus laurocerasus</i>	4.50	a	4.749	0.693	0.588	8.966	0.635	0.703
	<i>Viburnum tinus</i>	3.94	ab	3.749	0.582	0.623	20.684	0.912	0.747

D_{30} and species were significant predictors of the crown radius (R_{crown}) ($p < 0.001$). The best fitting between D_{30} and R_{crown} was obtained in both cities using a power function ($R_{crown} = a \times D_{30}^b$) with average R^2 of 0.439 and 0.545 in Lugano and Bolzano, respectively (Table 4). D_{30} and species were significant predictors of plant height (H_{tot}) ($p < 0.001$). The

power function ($H_{tot} = a \times D_{30}^b$) best-fitted the observed data in all species with an average R^2 of 0.381 and 0.499 in Lugano and Bolzano, respectively. The specific coefficient values and R^2 of both regressions, categorized by species and city, are shown in Table 4.

3.2. CO₂ Assimilation

3.2.1. CO₂ Assimilation per Unit Leaf Area

Photosynthesis of the different species was measured in sun and shaded leaves in Lugano and in Bolzano, during the different seasons. In Lugano, the net CO₂ assimilation per unit leaf area (A_{leaf} , $\mu\text{mol m}^{-2} \text{s}^{-1}$) significantly differed among species, seasons and leaf positions ($p < 0.001$). *Fi* and *Ee* showed higher A_{leaf} than *Ln*, *Lv*, and *Pl*. *Pl* had significantly lower A_{leaf} compared to all the other species investigated (Figure 1A). Apical external leaves (ae) had 6.94% higher A_{leaf} than basal external leaves (be). Shaded apical and basal leaves (ai and bi) had 60% and 83.2% lower A_{leaf} , respectively, compared to ae (Figure 1C). A_{leaf} declined in all species from spring to summer (−16.16%) and recovered in fall (+21.3% compared to summer) (Figure 1E).

In Bolzano, A_{leaf} was significantly affected by species and leaf position ($p < 0.001$) but not by season ($p = 0.241$). *Fi* and *Pt* showed higher A_{leaf} than all the other species investigated. *Pl* showed lower A_{leaf} than all the other species except for *Ej* (Figure 1B). A_{leaf} was similar in ae and be leaves. Ai and bi leaves had 51.7% and 77.5% lower A_{leaf} compared to ae (Figure 1D). Full data of A_{leaf} for each species, leaf position, season, and city can be found in Table A2 in Appendix A.

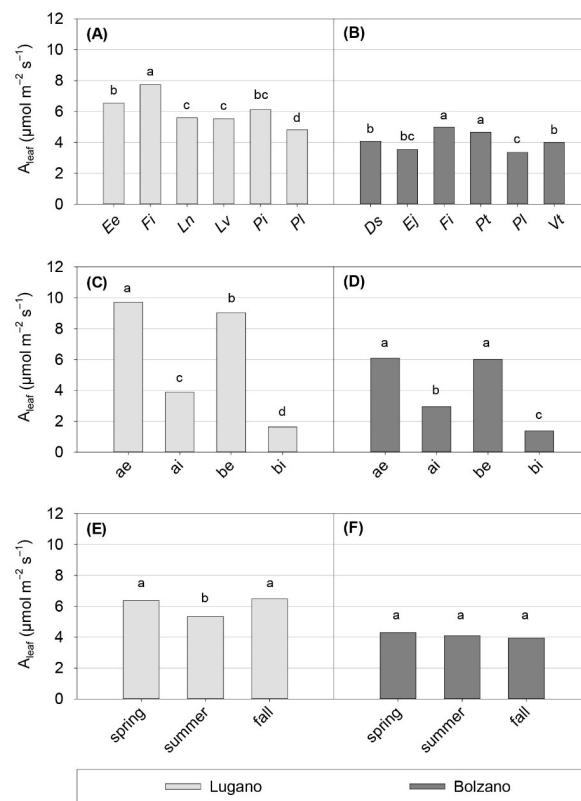


Figure 1. CO₂ assimilation per unit of leaf area (A_{leaf} , $\mu\text{mol CO}_2 \text{ m}^{-2} \text{ s}^{-1}$). Panels (A,B) show the effect of species, panels (C,D) show the effect of the leaf position on the crown, while panels (E,F) show the effect of season on the experimental cities of Lugano (A,C,E) and Bolzano (B,D,F). Within each panel, different letters indicate significant differences among species (A,B), among leaf positions (C,D) and between seasons (E,F) at $p \leq 0.05$. *Ds*: *Deutzia scabra*, *Ee*: *Elaeagnus × ebbingei*, *Ej*: *Euonymus japonicus*, *Fi*: *Forsythia × intermedia*, *Ln*: *Laurus nobilis*, *Lv*: *Ligustrum vulgare*, *Pl*: *Prunus laurocerasus*, *Pt*: *Pittosporum tobira*, *Vt*: *Viburnum tinus*.

3.2.2. CO₂ Assimilation per Unit Canopy Cover

In Lugano, the net hourly CO₂ assimilation per unit crown projection area at saturating irradiance (A_{cpa} , g m⁻² ground h⁻¹) was significantly affected by species ($p < 0.001$). Season ($p = 0.089$) and the interaction between species and seasons ($p = 0.948$) were not significant. *Ee*, *Fi*, and *Pt* had higher A_{cpa} than *Lv* (Figure 2A). A_{cpa} was about 14.3% higher in spring than in summer (Figure 2C).

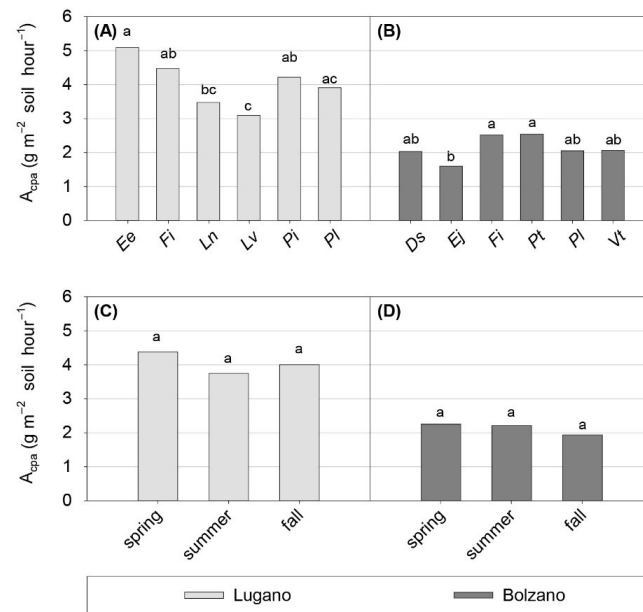


Figure 2. CO₂ assimilation per unit of crown projection area (A_{cpa} , g m⁻² h⁻¹). Panels (A,B) show the effect of species, while panels (C,D) show the effect of season, in the cities of Lugano (A,C) and Bolzano (B,D). Within each panel, different letters indicate significant differences between species (A,B) and between seasons (C,D) at $p \leq 0.05$. *Ds*: *Deutzia scabra*, *Ee*: *Elaeagnus × ebbingei*, *Ej*: *Euonymus japonicus*, *Fi*: *Forsythia × intermedia*, *Ln*: *Laurus nobilis*, *Lv*: *Ligustrum vulgare*, *Pt*: *Prunus laurocerasus*, *Pt*: *Pittosporum tobira*, *Vt*: *Viburnum tinus*.

In Bolzano, A_{cpa} was affected by species ($p < 0.001$), while season ($p = 0.122$) and the season × species interaction were not significant ($p = 0.506$). *Fi* and *Pt* displayed higher A_{cpa} compared to *Ej* (Figure 2B). A_{cpa} was about 13.8% higher in spring and summer than in fall (Figure 2D).

CO₂ assimilation per plant during an hour of saturating sunlight irradiance, calculated as the product of A_{cpa} and CPA , varied between 6.18 and 41.42 g plant⁻¹ h⁻¹ in Lugano and between 4.29 and 18.15 g plant⁻¹ h⁻¹ in Bolzano (Table 5).

3.3. Latent Heat Dissipation

3.3.1. Transpiration per Unit of Leaf Area

Transpiration and stomatal conductance of sun and shaded leaves of the different species were measured in different seasons in Lugano and in Bolzano. In Lugano, transpiration per unit leaf area (E_{leaf} , mmol H₂O m⁻² s⁻¹) was significantly affected by species, leaf position and season ($p < 0.001$). *Fi* displayed higher E_{leaf} than the other species evaluated (Figure 3A). *Pl* was the species with lower E_{leaf} and transpired 42.8% less water than *Fi*. All species experienced a temporary slight drop in E_{leaf} during summer (−14.9% compared to spring), then E_{leaf} fully recovered during fall. The interaction between species and leaf position was not statistically significant ($p = 0.094$).

In Bolzano, E_{leaf} was significantly affected by species, leaf position and season ($p < 0.001$). *Fi* showed 33% higher E_{leaf} than *Pl*. E_{leaf} of *Vt* and *Pt* did not differ from *Fi*. E_{leaf} increased by 42.8% from spring to summer, then dropped by 40.2% during fall

(Figure 3D). The interaction between the leaf position and the seasons was significant ($p = 0.01$).

Table 5. Average crown projection area (CPA_{avg} , m^2) and net CO_2 assimilation per plant (A_{plant} , $g\ plant^{-1}\ h^{-1}$) of the species investigated in Lugano and Bolzano.

		CPA_{avg}	A_{plant}
Lugano	Species	m^2	$g\ plant^{-1}\ h^{-1}$
	<i>Elaeagnus × ebbingei</i>	5.35	27.29
	<i>Forsythia × intermedia</i>	9.25	41.42
	<i>Laurus nobilis</i>	4.65	16.21
	<i>Ligustrum vulgare</i>	1.99	6.18
	<i>Pittosporum tobira</i>	6.19	26.15
	<i>Prunus laurocerasus</i>	4.87	19.10
Bolzano	Species	m^2	$g\ plant^{-1}\ h^{-1}$
	<i>Deutzia scabra</i>	3.35	6.84
	<i>Euonymus japonicus</i>	8.06	12.96
	<i>Forsythia × intermedia</i>	3.10	7.84
	<i>Pittosporum tobira</i>	7.11	18.15
	<i>Prunus laurocerasus</i>	6.22	12.81
	<i>Viburnum tinus</i>	2.36	4.89

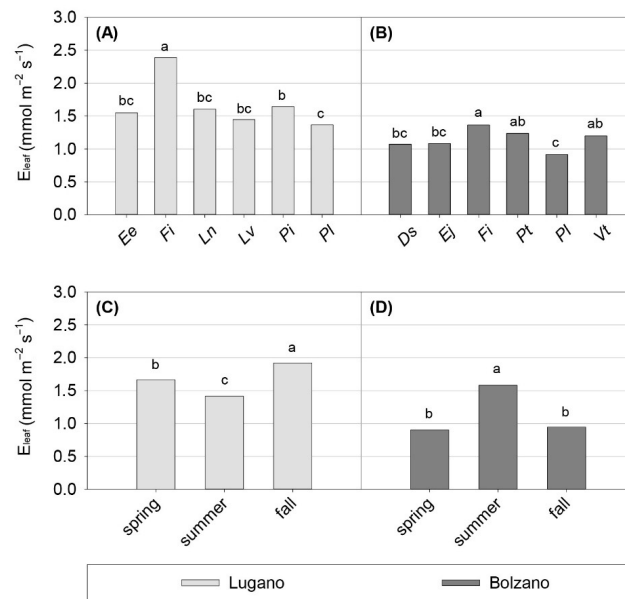


Figure 3. Transpiration per unit of leaf area (E_{leaf} , $mmol\ m^{-2}\ s^{-1}$) and latent heat dissipation per unit of crown projection area (LH_{cpa} , $W\ m^{-2}$). Panels (A,B) show the effect of species, while panels (C,D) show the effect of season, in the experimental cities of Lugano (A,C) and Bolzano (B,D). Within each panel, different letters indicate significant differences among species (A,B) and between seasons (C,D) at $p \leq 0.05$. Ds: *Deutzia scabra*, Ee: *Elaeagnus × ebbingei*, Ej: *Euonymus japonicus*, Fi: *Forsythia × intermedia*, Ln: *Laurus nobilis*, Lv: *Ligustrum vulgare*, Pl: *Prunus laurocerasus*, Pt: *Pittosporum tobira*, Vt: *Viburnum tinus*.

3.3.2. Latent Heat Dissipated per Unit Canopy Cover

In Lugano, the latent heat dissipated per unit crown projection area (LH_{cpa} , $W\ m^{-2}$) was significantly affected by the species ($p < 0.005$) and season ($p < 0.001$). The interaction between species and seasons was not significant ($p = 0.929$). Ee showed 27.7% higher LH_{cpa} than Ln (Figure 4A). LH_{cpa} was statistically similar in spring and summer, then it decreased by 32.2% in fall (Figure 4C).

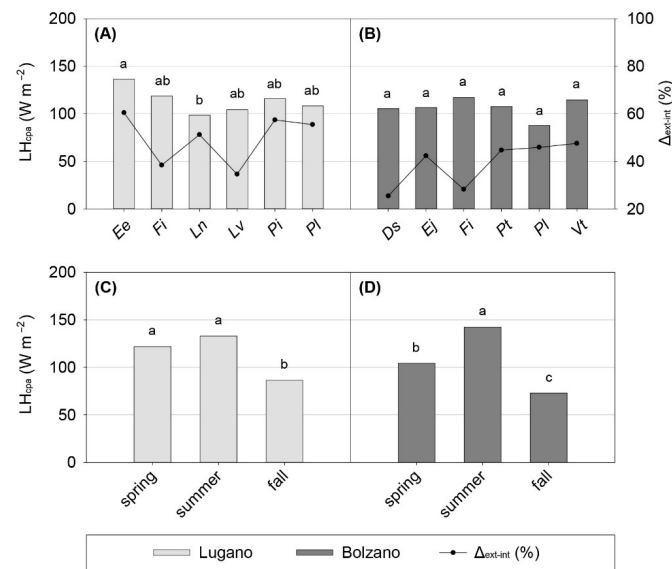


Figure 4. Latent heat dissipation per unit of crown projection area (LH_{cpa} , $W m^{-2}$). Panels (A,B) show the effect of species, while panels (C,D) show the effect of season, in the experimental cities of Lugano (A,C) and Bolzano (B,D). Within each panel, different letters indicate significant differences among species (A,B) and between seasons (C,D) at $p \leq 0.05$. The relative difference in LH_{cpa} between external and internal leaves across species is shown as $\Delta_{ext-int}$ (%) in panels (A,B) as a step line. Ds: *Deutzia scabra*, Ee: *Elaeagnus × ebbingei*, Ej: *Euonymus japonicus*, Fi: *Forsythia × intermedia*, Ln: *Laurus nobilis*, Lv: *Ligustrum vulgare*, Pt: *Pittosporum tobira*, Vt: *Viburnum tinus*.

In Bolzano, only season significantly affected LH_{cpa} ($p < 0.001$), while species ($p = 0.088$) and the interaction between species and seasons ($p = 0.946$) did not (Figure 4B). LH_{cpa} increased by 26.7% from spring to summer, and then it dropped by 48.7% in fall (Figure 4D).

3.4. Air Quality Amelioration

3.4.1. PM Accumulation and Deposition per Unit of Leaf Area

Particulate matter accumulated on leaves of the different species growing in Lugano and Bolzano was quantified. In Lugano, species affected the accumulation of $PM_{2.5-10}$ ($p = 0.008$). *Lv* accumulated 33% more $PM_{2.5-10}$ than *Fi* and *Ln*. No significant difference was observed among species for PM_{10-100} ($p = 0.160$) and $PM_{0.2-2.5}$ ($p = 0.173$) accumulation, with annual averages of $8.798 \mu g/cm^{-2}$ and $0.869 \mu g/cm^{-2}$, respectively (Figure 5A).

In Bolzano, species affected the accumulation of PM_{10-100} ($p < 0.001$) and $PM_{2.5-10}$ ($p = 0.001$), while the accumulation of $PM_{0.2-2.5}$ was unaffected ($p = 0.326$). The season of sampling significantly affected the accumulation of PM_{10-100} ($p = 0.042$) and $PM_{2.5-10}$ ($p < 0.001$), but did not affect the accumulation of $PM_{0.2-2.5}$ ($p = 0.096$). Evergreen species (*Ej*, *Pt*, *Pl*, and *Vt*) were 48% more efficient, on an annual basis, in PM_{10-100} accumulation than deciduous species (*Ds* and *Fi*). Moreover, *Ej* was found to be 35% more effective in accumulating $PM_{2.5-10}$ than *Ds* and *Fi* (Figure 5B). No interaction was observed between species and season for the accumulation of any PM fraction in either of the two cities studied, so species were not analyzed separately by season.

Species ($p = 0.006$) and season ($p = 0.030$) affected PM_{10} accumulation in Lugano, whereas species did not affect $depPM_{10}$ ($p = 0.115$). Lower PM_{10} accumulation was observed in spring compared to winter. In contrast, $depPM_{10}$ ($p < 0.001$) was higher in spring compared to summer, when, in turn, higher $depPM_{10}$ than in fall and winter was observed (Figure 6A,B). $PM_{2.5}$ accumulation ($p = 0.749$) was unaffected by season, while $depPM_{2.5}$ was significantly higher in spring ($p < 0.001$) (Figure 6C,D).

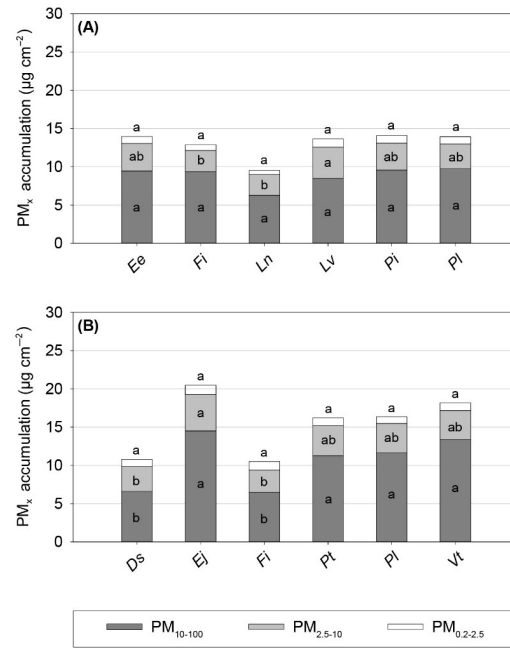


Figure 5. Effect of species on PM_{10-100} , $PM_{2.5-10}$, and $PM_{0.2-2.5}$ accumulation per unit leaf area ($\mu\text{g cm}^{-2}$) in Lugano (A) and Bolzano (B). Within each PM fraction, different letters indicate significant differences among species at $p \leq 0.05$. Ds: *Deutzia scabra*, Ee: *Elaeagnus × ebbingei*, Ej: *Euonymus japonicus*, Fi: *Forsythia × intermedia*, Ln: *Laurus nobilis*, Lv: *Ligustrum vulgare*, Pl: *Prunus laurocerasus*, Pt: *Pittosporum tobira*, Vt: *Viburnum tinus*.

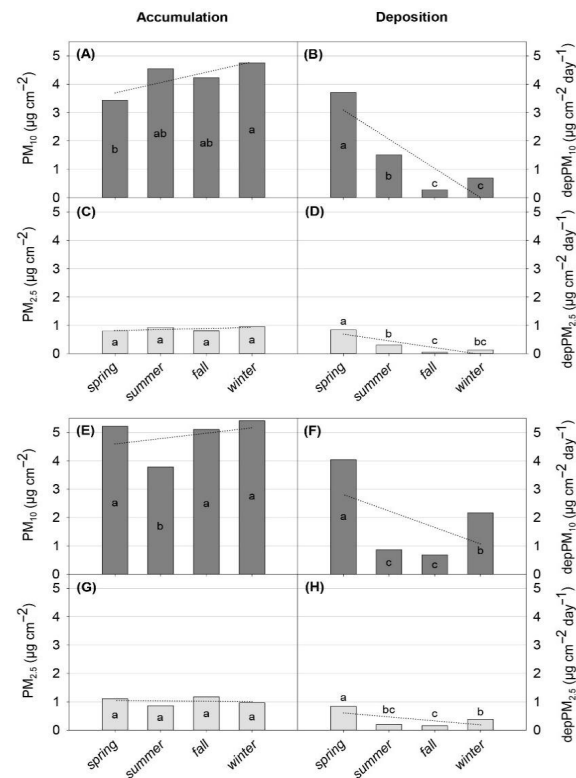


Figure 6. PM_{10} accumulation (A,E) and deposition (B,F) and $PM_{2.5}$ accumulation (C,G) and deposition (D,H) per unit leaf area in Lugano (A–D) and Bolzano (E–H). Within each variable, different letters indicate significant differences among seasons at $p \leq 0.05$. The dotted line represents the annual trend. Ds: *Deutzia scabra*, Ee: *Elaeagnus × ebbingei*, Ej: *Euonymus japonicus*, Fi: *Forsythia × intermedia*, Ln: *Laurus nobilis*, Lv: *Ligustrum vulgare*, Pl: *Prunus laurocerasus*, Pt: *Pittosporum tobira*, Vt: *Viburnum tinus*.

In Bolzano, the accumulations of PM_{10} , $depPM_{10}$, and $depPM_{2.5}$ were significantly affected by season ($p < 0.001$ for all traits). Species affected neither $depPM_{10}$ ($p = 0.131$) nor $depPM_{2.5}$ ($p = 0.318$). PM_{10} accumulation was lower in summer compared to all other seasons (Figure 6E). $depPM_{10}$ was higher in spring than winter, when, in turn, higher $depPM_{10}$ was observed compared to summer and fall (Figure 6F). The accumulation of $PM_{2.5}$ was unaffected by season, whereas $DepPM_{2.5}$ was higher in spring compared to other seasons (Figure 6G,H).

If total PM accumulation is compared between cities using data from the three species that were both in Lugano and Bolzano, *Pt* and *Pl* accumulated 14% more PM in Bolzano than in Lugano. Conversely, *Fi* accumulated 19% more PM in Lugano than in Bolzano.

Seasonal and annual accumulation and deposition values expressed per unit of leaf area for the different PM fractions by the six shrub species sampled in Lugano and Bolzano are provided in Appendix A.

3.4.2. PM Deposition per Unit Canopy Cover

In Lugano, PM_{10} deposition per unit crown projection area ($depPM_{10,cpa}$) was significantly affected by species ($p < 0.001$) and season ($p < 0.001$). *Ee* had significantly higher $depPM_{10,cpa}$ compared to *Ln*. $depPM_{10,cpa}$ was significantly higher in spring than in summer, when, in turn, higher $depPM_{10,cpa}$ was observed compared to fall and winter. $depPM_{2.5,cpa}$ was affected by season ($p < 0.001$), but was not affected by species ($p = 0.059$).

In Bolzano, species had no effect on $depPM_{10,cpa}$ ($p = 0.154$) or $depPM_{2.5,cpa}$ ($p = 0.457$). Conversely, the season significantly affected both $depPM_{10,cpa}$ and $depPM_{2.5,cpa}$ ($p < 0.001$).

Seasonal and annual deposition values expressed per unit canopy cover for both fractions by the six shrub species in Lugano and Bolzano are provided in Appendix A.

4. Discussion

4.1. CO₂ Removal from the Atmosphere

When estimated as CO₂ storage and sequestration, the capacity of shrubs to remove CO₂ is generally believed to be low, due to their small biomass at maturity [33,34]. In this research, CO₂ removal was estimated using a different approach that considers the photosynthetic capacity of the different species, as previously done with trees [4]. We conducted leaf gas exchange and Leaf Area Index measurements to calculate CO₂ assimilation per unit crown projection area (A_{cpa}). A_{cpa} is the net CO₂ uptake from the atmosphere (i.e., the photosynthetic CO₂ gain minus leaf autotrophic respiration) per unit canopy cover. Because shrubs are often planted and managed as masses rather than as individual plants, A_{cpa} may particularly be valuable for shrub species, since it provides an area-based metric for CO₂ uptake [34]. A_{cpa} of the shrub species investigated here ranged between 1.6 and 5.1 g CO₂ m⁻² ground h⁻¹, depending on species. One m² ground planted with *Fi*, *Pt*, *Ee*, *Ds* removed about 40% more carbon compared to the same ground area planted with *Ln*, *Lv*, *Ej*.

The main determinants of A_{cpa} are Leaf Area Index (*LAI*) and net photosynthetic rate per unit leaf area [35]. Shrubs often display high canopy density, which can be further increased when they are regularly pruned [30,36], as it occurs in most municipalities [37]. High canopy density can result in similar *LAI* in shrubs compared to trees, although canopy height is substantially lower [36]. Consistently, shrub species investigated here displayed, on average, 10% higher *LAI* compared to tree species growing in similar climates [4]. Dense canopies with *LAI* > 4.5 were found in *Ee*, *Pl*, and *Pt*, especially when grown in Lugano, where high rainfall during sprouting may have favored shoot growth [38,39]. Increasing *LAI* enhances photosynthetic area per unit ground area, but the amount of canopy subjected to self-shading and shade intensity increases as well [35]. Plants can acclimate the morpho-

anatomy and physiology of their leaves to maintain a positive carbon balance in shade, although the capacity to acclimate depends on species and shade density [40,41]. As an example, the contribution of shaded leaves to overall canopy photosynthesis was 7% lower in Lugano than in Bolzano, because the denser canopies in the former city reduced light penetration to the inner canopy.

The contribution of shaded leaves to canopy photosynthesis did not significantly differ among species, although photosynthetic rate per unit leaf area did. *Fi*, a fast-growing deciduous species with thick palisade tissue and high chlorophyll levels [42], had higher photosynthesis per unit leaf area than most of the other species in both cities. Such a difference may be due to lower diffusive limitations to photosynthesis and to higher nitrogen allocation to the photosynthetic apparatus occurring in deciduous than in evergreen species [43]. The 37% difference in A_{leaf} observed in *Fi* between Lugano and Bolzano suggests opportunistic water use by *Fi*, which maximizes photosynthesis under high moisture availability and strictly modulates stomatal opening to avoid dehydration in drier conditions [44]. *Pt*, an evergreen heat-tolerant Mediterranean species with a more conservative water-use [44], was as effective as *Fi* for CO₂ assimilation when planted in the drier conditions of Bolzano. At the other end of the spectrum, *Pl*, a species known for its high stomatal sensitivity to moisture availability and high hydraulic limitations under water stress [45], displayed the lowest photosynthetic rate among the species investigated in both cities. The A_{leaf} values observed in this research were consistent with previous literature [45–47], although we found that A_{leaf} was, in general, lower in Bolzano than in Lugano. Such a result was unexpected, because the cities fall within the same climatic zone, but it may be due to higher soil pH in Bolzano than in Lugano and to the differing total annual rainfall and rainfall distribution between the cities. Although total rainfall was 40% lower in Bolzano than in Lugano, the latter city experienced a relatively dry summer, which did not occur in Bolzano, where summer rainfall exceeded the 30-year average by 36%.

Modeling the change in whole-plant net CO₂ assimilation as a function of plant age or stem diameter, as previously done with tree species [4], may be of little practical significance and subject to high uncertainty in shrubs for several reasons: (1) stem diameter of shrubs are seldom measured and recorded in municipal inventories [48]; (2) criteria for stem diameter measurement are often inconsistent among municipalities and tree workers, because shrubs are usually multi-stemmed and branched below 1.3 m [23]; (3) stem diameter may be a poor predictor of crown projection area and plant height in shrubs, as displayed by the low R² of the allometric relationship obtained here, because crown radius and height were greatly affected by planting distances, planting layout, and pruning regime [49]. On average, shrubs measured in this research assimilated 6.2 to 41.4 g CO₂ h⁻¹ plant⁻¹ in Lugano and 4.9 to 18.2 g CO₂ h⁻¹ plant⁻¹ in Bolzano. This is 97.8% lower than trees under a similar climate [4]. However, such a large difference between trees and shrubs is mostly due to differences in canopy size. Indeed, when estimated per square meter of canopy cover, CO₂ assimilation of shrubs accounted for 23.6% of that observed in tree species in a similar climate zone [4]. This indicates that CO₂ uptake by the urban forest can be increased by designing multi-layered green areas which integrate a shrub layer made of species with high A_{cpa} , as also suggested by [34].

4.2. Latent Heat Dissipation

Only a few studies evaluated the capacity of shrubs to improve the microclimate. Most of these studies assessed microclimate amelioration by measuring temperature using infrared or remote sensing [50,51]. In this study, latent heat dissipation (LH_{cpa} , W m⁻²) was evaluated using a Penman–Monteith approach based on direct measurements of leaf gas exchange. LH_{cpa} by shrubs ranged between 87 and 136 W m⁻² over the 24 h, depending

on the species. The latent heat dissipation by *Ln* was approximately one-third that of the same surface area planted with *Ee* (Figure 4A,B). Main determinants of LH_{cpa} are stomatal and aerodynamic resistances to transpiration, weather parameters and LAI.

Transpiration per unit of leaf area (E_{leaf}) differed significantly among species in both cities. *Fi* had the highest transpiration rate of the investigated species and transpired 52.3% more water than *Pl*, the species with the lowest transpiration rate. In Lugano, *Fi* outperformed other species in terms of E_{leaf} . The 54% difference in E_{leaf} observed for *Fi* between Lugano, characterized by higher total annual rainfall, and Bolzano confirms its opportunistic water use, which maximizes stomatal opening under higher water availability, but strongly regulates water loss during heat and drought stress. In contrast, *Pt*, a species characterized by a more conservative water use, showed only 14% variation in E_{leaf} between the two cities despite their different microclimatic conditions during the measurements [44]. Regardless of the city, E_{leaf} measured in this experiment were lower than those found on well-watered plants of the same species [45–47,52] and were similar to those found on *Fi*, *Ln*, *Pt* and *Vt* in studies under drought stress in pot-grown plants [46,53].

The results of this experiment indicate how differences in LAI and canopy density among species can affect cooling capacity. Transpiring leaf area per ground square meter increases indeed with LAI, with positive effects on cooling. Thus, species with high LAI, such as *Ee*, were extremely effective in cooling, although their E_{leaf} was relatively low. Conversely, low LAI prevented *Fi* from providing higher LH_{cpa} than most of the other species, despite its higher E_{leaf} . On the other hand, light transmittance to the inner canopy decreases with increasing LAI, thus increasing the relative amount of leaves subjected to self-shading while decreasing the irradiance reaching shaded leaves (Appendix A). As a consequence, shaded leaves of the high-LAI species *Ee* transpired 60% less water than their full-sun counterparts, whereas transpiration of shaded leaves of the sparse-canopy low-LAI *Lv* was only 34% lower than full-sun leaves.

LH_{cpa} increased with temperature and vapor pressure deficit (VPD), being higher in summer and lower in fall. This underlines the high potential for cooling of shrubs, which were capable of higher latent heat dissipation when it is more beneficial to the population. Apart from temperature, the drop of LH_{cpa} in fall may be associated with a higher frequency of self-shaded leaves within the canopy, due to wider solar zenith angle.

Schwaab et al. [54] showed how green spaces with trees cool down 2–4 times more than treeless green spaces. Latent heat fluxes around 100–200 W m⁻² are reported in the literature for urban trees, measured both with direct [30,55] and indirect [56] methods. We show here that the latent heat flux by the shrub species investigated was in the same order of magnitude as that of trees. Thus, although shrubs are much less effective at casting shade than trees, because of their smaller size [30], their capacity to dissipate latent heat through transpiration should not be underestimated.

4.3. Particulate Matter Removal

Although bark contributes to PM capture, leaves are the main plant organs responsible for atmospheric PM accumulation [57]. Leaf micromorphological traits, such as trichomes, stomata, and epicuticular waxes, are often linked to higher PM retention [58–60]. Baraldi et al. [61] used Scanning Electron Microscopy to examine *Ligustrum* spp., revealing peltate trichomes, waxes, and cuticular characteristics (ridges, grooves, prominent stomata, and irregular wax deposits), which may explain the higher $PM_{2.5-10}$ and PM_{10} accumulation observed in *Lv* in Lugano. In the same study [61], *Ln* showed a stomatal density similar to *Ligustrum* spp. (200–300 stomata per mm²) but lacked trichomes. While higher stomatal density is generally linked to greater PM adsorption on leaves [62], the absence of additional contributing factors in *Ln* may explain its low PM accumulation in Lugano. This trend

was also confirmed by other studies, where *Ln* was among the least efficient species in capturing PM [63]. *Ee*, which showed intermediate $PM_{2.5-10}$ and PM_{10} accumulation in Lugano, was identified by Mori et al. [63] as the most efficient species in PM capture due to high leaf area, biomass, and favorable leaf traits like trichomes [6]. *Fi* was among the least efficient species for $PM_{2.5-10}$ and PM_{10} accumulation in Lugano and also performed poorly in Bolzano, including for PM_{10-100} . Dzierzanowski et al. [64] found that *Fi* leaves had 2 to 8 times more waxes than other species analyzed; however, this did not significantly enhance PM retention. The potential of epicuticular waxes to trap PM depends on their chemical composition and structure, which vary depending on species [65]. Additionally, *Fi* lacks ultrastructures, such as thin films and tubules, that promote PM accumulation [65], potentially explaining its low efficiency observed in this study.

Macroscopic leaf properties (e.g., shape and size) and canopy structure can impact leaf PM accumulation capacity [60,66], interacting with climatic and environmental factors [67]. Leaf density within the canopy also significantly affects PM adsorption. In Lugano, *Lv* had the highest PM accumulation but the lowest LAI (33% below the average of other species). Such a result may be explained by the micro-turbulence generated in porous canopies, which can enhance $PM_{2.5-10}$ and PM_{10} capture. Canopy density influences wind turbulence, a key factor for PM deposition, especially fine particles [68]. Excessive leaf density reduces canopy porosity, limiting airflow and consequently its filtering effect [69,70]. Similarly, in Bolzano, *Ej*, which had 20% lower LAI than the other species analyzed, showed high accumulation of PM_{10-100} , $PM_{2.5-10}$, and PM_{10} . As with *Lv* in Lugano, higher canopy porosity in *Ej* likely enhanced PM capture.

Evergreen species capture PM throughout the year, including winter when air PM levels are higher, unlike deciduous species that shed their leaves annually. However, since evergreens retain their leaves for years, they may accumulate less new particulate matter each season [58,71]. In Bolzano, *Vt* was highly efficient in capturing PM_{10-100} per unit of leaf area, consistently with previous research [63]. This efficiency is likely due to its abundant wax layer [61] and a dense trichome indumentum, which enhances PM retention.

Comparing the cumulative adsorption of the three species grown in both Lugano and Bolzano with the atmospheric PM concentrations during the sampling and pre-sampling periods in both cities, some trends emerged. The use of evergreen species such as *Pt* may be particularly effective in sites where air PM concentration peaks during winter, as was the case in Bolzano. In contrast, deciduous species can be used effectively when the peak in air PM concentration occurs during the growing season, such as in Lugano.

Meteorological and environmental factors can influence the complex process of accumulation, wash-off and re-suspension of PM [72,73]. In both Lugano and Bolzano, PM_{10} accumulation increased over the year, coherently with previous studies [74,75]. This is probably linked to higher winter air PM concentrations, primarily due to heating-related combustion. High winter accumulation is also attributed to wet leaf surfaces and fog, which favor wet deposition [76,77]. While high pollution levels can promote leaf PM accumulation [78,79], heavy rain and strong winds can wash off or resuspend accumulated PM [80]. In Bolzano, summer rain corresponded to the lowest leaf accumulation, while in Lugano, spring rainfall likely washed away PM, explaining lower accumulation in that season. The high PM accumulation on leaves observed in Bolzano can be explained by the dominance of evergreen species in the sample, which capture PM year-round, and by much less rainfall experienced by that city during spring, compared to Lugano [81]. Deciduous species, which shed leaves, tend to capture less PM and, among them, those that retain their leaves for longer periods are more efficient.

The opposite seasonal trend of accumulation and deposition (both per unit of leaf area and per unit canopy cover) supports the idea that particulate matter is primarily adsorbed

onto specific leaf microstructures (e.g., cuticular characteristics, trichomes, glands, etc.) [59]. As these microstructures become saturated, the deposition rate decreases [82], resulting in fewer particles that can accumulate daily on leaf surfaces that are nearing saturation.

4.4. Limitations

In this research, net photosynthetic rate, stomatal conductance and PM accumulation measured per unit leaf area were upscaled to calculate the benefits provided by some shrub species. We independently measured photosynthesis and stomatal conductance in sun and shaded leaves to upscale the data using a sun–shade model, which is more accurate than the traditional big-leaf model [12]. Nonetheless, we are aware that the estimation of CO₂ assimilation and latent heat dissipation per unit crown projection area relies on strong assumptions in the upscaling procedure. Similarly, the methods to calculate the PM deposition relied on the assumption that a rainfall event with intensity >7 mm could completely wash off PM from leaves.

5. Conclusions

This research shows that, although their benefits per plant are inextricably lower than in tree species because of smaller size, shrubs can provide significant ecosystem services in terms of CO₂ assimilation, latent heat dissipation, as well as accumulation and deposition of atmospheric particulate matter (PM). Per m² of crown projection area, shrubs dissipated up to 130 W m⁻² latent heat per day and assimilated up to 5 g CO₂ m⁻² ground h⁻¹ of full sun, which can be comparable to tree species. Moreover, shrubs were efficient filters for particulate matter due to their growth form, indicating possible benefits of planting them near roads, one of the most significant emission sources. Nonetheless, the provision of such benefits varies between species, emphasizing the need for a science-based design of urban vegetation that takes into account the capacity of a given species to provide the desired benefit.

Author Contributions: Conceptualization, P.V., F.F. and A.F.; methodology, S.C., D.C., I.V., and A.F.; formal analysis, S.C., D.C., and I.V.; investigation, S.C., C.V., and A.F.; resources C.V., C.B., and E.C.; data curation, S.C., D.C., I.V., and A.F.; writing—original draft preparation, S.C., D.C., and I.V.; writing—review and editing, P.V., F.F. and A.F.; visualization, S.C., D.C., and I.V., supervision, F.F. and A.F.; project administration, P.V.; funding acquisition, C.V., C.B., E.C., and P.V. All authors have read and agreed to the published version of the manuscript.

Funding: This research was funded by the program Interreg V-A Italy-Switzerland 2014–2020, Axis 1: Business Competitiveness, through the VERDEVALE project (Project ID 640221, CUP E31C18000090004), co-financed by the European Union (ERDF), the Italian State, the Swiss Confederation, and the Cantons.

Data Availability Statement: The raw data supporting the conclusions of this article will be made available by the authors on request.

Acknowledgments: The authors are grateful to Alice Gazzoli for the help during the measurement campaigns. No AI was used in preparing the manuscript.

Conflicts of Interest: Author Paolo Viskanic is employed in the company R3 GIS S.r.l. The remaining authors declare that the research was conducted in the absence of any commercial or financial relationships that could be construed as a potential conflict of interest. The funders had no role in the design of the study; in the collection, analyses, or interpretation of data; in the writing of the manuscript; or in the decision to publish the results. Francesco Ferrini, being both an author of this manuscript and an editor of the *Urban Science* journal, declares that he will have no role in the review process and will not influence reviewers' decisions and opinions in any way.

Abbreviations

The following abbreviations are used in this manuscript:

ae	Apical external leaves
ai	Apical internal leaves
A_{cpa}	Net hourly CO ₂ assimilation per unit crown projection area
A_{leaf}	Net CO ₂ assimilation per unit leaf area
A_{plant}	Net hourly CO ₂ assimilation by an individual plant
be	Basal external leaves
bi	Basal internal leaves
CPA	Crown projection area
D_{30}	Stem diameter measured at 30 cm height
D_{tot}	Cumulated stem diameter of multi-stemmed plants
E_{leaf}	Transpiration per unit leaf area
ES	Ecosystem services
g_s	Stomatal conductance to water vapor
LAI	Leaf Area Index
LAI_{sun}	Fraction of LAI exposed to full sun at a given solar zenith angle
LAI_{shade}	Fraction of LAI subjected to self-shading at a given solar zenith angle
LH_{cpa}	Latent heat dissipation
PAI_e	Effective Plant Area Index
PAR	Photosynthetic active radiation
PAR_{sun}	PAR experienced by external leaves
PAR_{shade}	PAR experienced by internal leaves
PM	Particulate matter
R_{crown}	Crown radius
WAI	Woody Area Index
θ	Solar zenith angle
Ω	Clumping index

Appendix A

- LAI partitioning into the sun and shade fraction

According to the multilayer approach, the crown was divided into two layers: sunny leaves and shaded leaves [29]. These two layers were again divided into two groups, apical and basal, assuming the equal vertical distribution of leaves in the crown. The LAI was also partitioned into its two sun and shaded fractions.

$$LAI_{sun_a} = 2\cos\theta \times (1 - e^{-0.5 \times \Omega \times (LAI/2)/\cos\theta})$$

$$LAI_{sun_b} = 2\cos\theta \times (1 - e^{-0.5 \times \Omega \times (LAI/2)/\cos\theta})$$

$$LAI_{shade_a} = \frac{LAI}{2} - LAI_{sun_a}$$

$$LAI_{shade_b} = \frac{LAI}{2} - LAI_{sun_b}$$

$$LAI = LAI_{sun_a} + LAI_{sun_b} + LAI_{shade_a} + LAI_{shade_b}$$

where θ is solar zenith angle (rad), and Ω is the clumping index, i.e., the aggregation of leaves around branches and plant crowns. Ω was considered as a single average value not varying along the vertical profile of the whole canopy and calculated according to the equation found by [29].

- Net CO₂ assimilation upscaling

Values of photosynthesis were obtained with punctual measurement, using saturating light for external leaves. To avoid overestimation, the upscaling of net CO₂ assimilation per unit of crown projection area (A_{cpa} , g m⁻² ground⁻¹ h⁻¹) was limited to one hour of saturating light. In order to upscale to values per day, daily measurements were needed [4]. A_{cpa} was obtained by upscaling the net CO₂ assimilation per unit leaf area to the whole crown using a multilayer approach [4] on a daily basis, as follows:

$$A_{cpa_hour} = [0.5 \times (A_{ae} \times LAI_{sun_a} + A_{ai} \times LAI_{shade_a}) + 0.5 \times (A_{be} \times LAI_{sun_b} + A_{bi} \times LAI_{shade_b})] \times 44 \times 10^{-6} \times 3600$$

where A_{cpa_hour} is the total net CO₂ assimilation by the leaves covering a square meter of crown area, respectively, during one hour of saturating light. A_{ae} , A_{ai} , A_{be} and A_{bi} are the net CO₂ assimilation per unit leaf area (μmol m⁻² s⁻¹) of ae, ai, be and bi leaves, respectively, in spring, summer and fall (see Table A2 for full data). LAI_{sun} and LAI_{shade} are the fractions of LAI fully exposed to solar irradiance and self-shaded, respectively, assessed on a daily basis for each season; 0.5 is a coefficient for considering an equal distribution of leaf area between the apical and basal canopy layers; 44×10^{-6} is a coefficient to convert CO₂ from μmol to g, while 3600 represents the number of seconds in one hour.

- Latent heat dissipation through transpiration

The latent heat flux due to transpiration λT_c (W m⁻²) was calculated on a daily basis, according to [31]

$$\lambda T_c = \frac{\Delta Q + \rho_a C_p \frac{VPD}{R_a}}{\Delta + \gamma \left(1 + \frac{R_s}{R_a}\right)}$$

where Q (available energy) = R_n (mean net radiation) – G (soil heat flux); ρ_a is the mean air density at constant pressure; C_p is the specific heat of air; and Δ represent the slope of the saturation vapor pressure–temperature relationship, calculated as:

$\Delta = 4098 \left(0.6108 e^{(17.27 T)/(T+237.3)}\right) / (T + 237.3)^2$ where T is the air temperature (FAO); γ is the psychrometric constant γ (kPa °C) = $0.665 \times 10^{-3} * P$, where P is the air pressure (kPa); VPD is the vapor pressure deficit of the air (kPa); R_a is the aerodynamic resistance and R_s is the surface resistance.

R_a can be described as the resistance from the vegetation upward and involves friction from air flowing over vegetative surfaces. R_a was calculated between the top of the trees and a reference point (z) where the measurements of weather variables were carried out according to Rana et al. [31]. This method introduces two simplifying assumptions regarding the homogeneity of the transpiration layer: R_a was assumed to be the same for the whole tree canopy and for all trees of the same species.

$$R_a = \frac{\log\left(\frac{z-d}{z_0}\right) \log\left(\frac{z-d}{h_t}\right)}{k^2 u_z}$$

where d (m) is the zero-plane displacement and is estimated as $d = 0.67h_t$; h_t (m) is the mean height of trees; k is the von Kármán constant (0.40); U_z is the wind speed (m s⁻¹), measured at the reference point z above the canopy; and z_0 (m) is the roughness length estimated by $z_0 = 0.1 h_t$.

The methods used for canopy resistance (R_s) parametrization differed from Rana et al. [31]. R_s represents the resistance of vapor flow through the transpiring vegetation, hence through stomata opening, and it can also be perceived as the inverse of the canopy conductance ($1/g_{s,canopy}$).

The unit of measure of g_{sw} is converted from $\text{mmol m}^{-2} \text{s}^{-1}$ to ms^{-1} . Therefore, the canopy conductance ($g_{s,canopy}$) is estimated for each canopy layer (sun/shade and apical/basal), upscaling the leaf stomatal conductivities (g_{sw_ai} , g_{sw_ae} , g_{sw_bi} , g_{sw_be} , $\text{mmol m}^{-2} \text{s}^{-1}$) with its specific LAI fraction (LAI_{sun_a} , LAI_{sun_b} , LAI_{shade_a} and LAI_{shade_b} ; 2.3.1). R_s was obtained, for each fraction, as: $R_s = 1/g_{s,canopy} \cdot LH_{cpa_day}$ is then obtained with equation 1 using these within-fraction values. This process is repeated using the environmental condition and the leaf stomatal conductivity measured at night (LH_{cpa_night}). Finally, LH_{cpa} is calculated as:

$$LH_{cpa} = LH_{cpa_day} + LH_{cpa_night}$$

$$LH_{cpa_day} = LH_{sun_a_day} + LH_{shade_a_day} + LH_{sun_b_day} + LH_{shade_b_day}$$

$$LH_{cpa_night} = LH_{sun_a_night} + LH_{shade_a_night} + LH_{sun_b_night} + LH_{shade_b_night}$$

Table A1. The table reports the PAR values measured on apical and basal external (“ae” and “be”) and internal (“ai” and “bi”) leaves in Lugano (a) and Bolzano (b). The crown transmittance (τ), calculated as PARin/PARout, is separately reported for apical (τ_a) and basal (τ_b) leaves.

		(a)					
Lugano		<i>Elaeagnus</i> \times <i>ebbingei</i>	<i>Forsythia</i> \times <i>intermedia</i>	<i>Laurus</i> <i>nobilis</i>	<i>Ligustrum</i> <i>vulgare</i>	<i>Pittosporum</i> <i>tobira</i>	<i>Prunus</i> <i>laurocerasus</i>
Spring	ae	1297.25	1294.44	1300.13	1298.25	1296.67	1293.33
	ai	406.63	561.44	385.50	492.75	378.11	356.44
	τ_a	0.31	0.43	0.30	0.38	0.29	0.28
	be	1298.13	1300.22	1297.75	1295.00	1298.78	1299.67
	bi	74.75	90.44	142.13	178.88	87.00	50.22
	τ_b	0.06	0.07	0.11	0.14	0.07	0.04
Summer	ae	1295.63	1295.33	1299.00	1298.63	1296.89	1298.00
	ai	441.63	469.78	397.00	464.25	369.89	350.67
	τ_a	0.34	0.36	0.31	0.36	0.29	0.27
	be	1294.63	1297.89	1300.00	1299.38	1296.89	1299.78
	bi	85.00	90.56	153.25	133.50	63.11	50.11
	τ_b	0.07	0.07	0.12	0.10	0.05	0.04
Fall	ae	1296.00	1295.22	1299.38	1292.00	1295.44	1294.89
	ai	469.13	544.56	451.50	537.00	427.89	416.33
	τ_a	0.36	0.42	0.35	0.42	0.33	0.32
	be	1298.63	1300.33	1297.38	1298.38	1298.89	1296.67
	bi	85.38	101.33	165.00	151.75	72.00	54.33
	τ_b	0.07	0.08	0.13	0.12	0.06	0.04
		(b)					
Bolzano		<i>Deutzia</i> <i>scabra</i>	<i>Euonymus</i> <i>japonicus</i>	<i>Forsythia</i> \times <i>intermedia</i>	<i>Pittosporum</i> <i>tobira</i>	<i>Prunus</i> <i>laurocerasus</i>	<i>Viburnum</i> <i>tinus</i>
Spring	ae	1298.43	1298.00	1296.14	1294.57	1294.29	1297.00
	ai	454.29	274.43	401.14	245.14	219.14	187.00
	τ_a	0.35	0.21	0.31	0.19	0.17	0.14
	be	1293.00	1295.14	1300.57	1299.14	1292.29	1300.14
	bi	175.00	90.43	156.86	86.86	56.14	83.29
	τ_b	0.14	0.07	0.12	0.07	0.04	0.06

Table A1. Cont.

		(b)					
Bolzano		<i>Deutzia scabra</i>	<i>Euonymus japonicus</i>	<i>Forsythia × intermedia</i>	<i>Pittosporum tobira</i>	<i>Prunus laurocerasus</i>	<i>Viburnum tinus</i>
Summer	ae	1295.63	1298.00	1297.63	1298.38	1296.00	1297.50
	ai	395.50	304.50	322.50	277.25	239.88	268.50
	τ_a	0.31	0.23	0.25	0.21	0.19	0.21
	be	1301.63	1302.38	1298.63	1297.50	1297.63	1294.25
	bi	121.75	154.75	100.88	82.25	58.00	86.50
	τ_b	0.09	0.12	0.08	0.06	0.04	0.07
Fall	ae	1296.50	1298.50	1295.25	1294.25	1296.43	1299.88
	ai	295.00	203.25	254.38	171.63	159.71	186.88
	τ_a	0.23	0.16	0.20	0.13	0.12	0.14
	be	1296.88	1296.75	1297.75	1296.75	1297.71	1293.88
	bi	99.25	84.13	94.00	53.63	52.00	60.38
	τ_b	0.08	0.06	0.07	0.04	0.04	0.05

Table A2. The stomatal conductance to water vapor (g_{sw} ; $\text{mmol H}_2\text{O m}^{-2} \text{s}^{-1}$) and the net CO_2 assimilation per unit of leaf area (A ; $\mu\text{mol CO}_2 \text{m}^{-2} \text{s}^{-1}$) in different leaf positions and different seasons for each city. ae = apical external; be = basal external; ai = apical internal and bi = basal internal.

	gsw											
	Spring				Summer				Fall			
	ae	ai	be	bi	ae	ai	be	bi	ae	ai	be	bi
Lugano												
<i>Elaeagnus × ebbingei</i>	135.00	61.88	119.13	44.25	116.00	46.00	106.25	31.13	173.50	73.50	178.00	48.13
<i>Forsythia × intermedia</i>	229.56	134.44	201.78	102.78	132.00	112.11	149.22	59.11	215.11	140.11	205.56	131.89
<i>Laurus nobilis</i>	142.38	68.13	144.88	72.00	103.50	55.50	94.88	40.00	150.00	77.50	118.63	62.00
<i>Ligustrum vulgare</i>	98.63	80.38	104.63	67.63	95.38	51.13	70.13	45.13	137.50	94.13	102.38	71.50
<i>Pittosporum tobira</i>	152.56	57.00	151.22	44.22	100.44	58.89	100.44	38.67	133.78	51.89	139.22	42.78
<i>Prunus laurocerasus</i>	106.56	64.33	109.33	49.44	82.33	42.56	74.78	25.56	124.67	49.44	106.44	46.67
Bolzano												
<i>Deutzia gracilis</i>	63.57	65.14	66.57	47.43	49.00	43.63	59.25	42.38	81.25	81.88	89.63	71.88
<i>Euonymus japonicus</i>	53.86	38.00	47.86	38.14	59.75	39.63	69.88	26.13	71.63	46.00	58.75	42.00
<i>Forsythia × intermedia</i>	58.29	60.14	84.57	53.29	77.88	72.50	119.25	56.88	66.75	83.50	99.25	73.50
<i>Pittosporum tobira</i>	66.71	47.43	48.00	21.43	72.38	55.13	80.38	41.38	113.50	58.00	81.50	27.13
<i>Prunus laurocerasus</i>	54.57	42.43	44.86	25.71	62.63	46.38	65.25	23.75	56.71	41.86	68.29	37.14
<i>Viburnum tinus</i>	77.14	42.71	76.14	41.43	70.63	44.25	70.38	34.63	76.63	52.50	80.75	30.00

Table A2. Cont.

Lugano	A											
	Spring				Summer				Fall			
	ae	ai	be	bi	ae	ai	be	bi	ae	ai	be	bi
<i>Elaeagnus</i> × <i>ebbingei</i>	11.40	3.28	9.78	1.44	10.05	3.33	8.39	1.13	12.23	3.76	13.05	1.39
<i>Forsythia</i> × <i>intermedia</i>	12.42	6.41	12.39	2.57	9.86	6.02	10.99	1.32	12.41	4.97	11.14	2.46
<i>Laurus nobilis</i>	8.65	3.88	9.15	1.44	8.06	3.33	7.35	1.89	8.89	3.18	7.64	2.35
<i>Ligustrum vulgare</i>	7.74	4.51	8.28	3.09	7.41	2.95	5.51	1.78	11.01	5.71	8.19	2.33
<i>Pittosporum tobira</i>	10.28	3.32	10.64	1.36	8.91	3.54	8.32	1.22	10.79	3.58	9.98	1.58
<i>Prunus laurocerasus</i>	8.76	3.23	8.58	0.72	7.76	2.66	6.12	0.71	8.47	2.49	7.44	0.90
Bolzano	ae	ai	be	bi	ae	ai	be	bi	ae	ai	be	bi
<i>Deutzia gracilis</i>	6.77	4.67	6.04	2.43	4.49	2.98	5.23	1.58	4.99	2.63	5.35	1.25
<i>Euonymus japonicus</i>	5.29	2.44	4.86	1.14	5.08	2.21	5.60	0.89	5.89	2.18	5.13	1.13
<i>Forsythia</i> × <i>intermedia</i>	5.99	4.21	7.36	2.44	7.89	3.89	9.04	1.59	5.58	3.39	6.28	1.66
<i>Pittosporum tobira</i>	6.76	3.16	5.14	1.23	6.83	3.60	7.03	1.48	8.81	3.08	7.06	1.06
<i>Prunus laurocerasus</i>	5.27	2.53	4.19	0.74	5.26	2.74	5.10	0.86	4.71	1.77	5.46	0.86
<i>Viburnum tinus</i>	6.73	1.69	6.57	1.43	6.05	2.18	5.43	1.13	6.41	2.58	6.24	0.84



Figure A1. Images of the experimental areas in Lugano (right) and Bolzano (left). The red perimeters identify the experimental areas: the numbers identify the plots as inventoried in the municipal tree inventory database. In Lugano, block 1 was made by plots 2004 and 2016, block 2 by 5053, block 3 by 6007 and 6024, block 4 by 8021 and 8007, block 5 by 5019, block 6 by 8009, block 7 by 5055, block 8 by 6005 and block 9 by plot 2012. In Bolzano, block 1 was made by plot 6666, block 2 by 309, block 3 by 9121 and 5077, block 4 by 4260 and 1891, block 5 by 9207, 9307 and 9211, block 6 by 3490 and 9124, block 7 by 5130, 8550 and 9001 and block 8 by plot 3103 and 9114.

Table A3. Seasonal and annual accumulation (PM_x ; $\mu\text{g cm}^{-2}$ leaf area) and deposition ($depPM_x$; $\mu\text{g cm}^{-2} \text{day}^{-1}$) expressed per unit of leaf area for the different PM fractions by the six shrub species in Lugano (a) and Bolzano (b).

(a)					
Species	PM ₁₀₋₁₀₀ ($\mu\text{g cm}^{-2}$)				
	Spring	Summer	Fall	Winter	Annual Average
<i>Elaeagnus × ebbingei</i>	3.436	8.43	12.916	13.08	9.466
<i>Forsythia × intermedia</i>	5.981	8.478	13.598	-	9.352
<i>Laurus nobilis</i>	1.728	6.065	8.295	9.117	6.301
<i>Ligustrum vulgare</i>	5.109	8.565	12.469	7.778	8.48
<i>Pittosporum tobira</i>	5.684	8.658	12.385	11.561	9.572
<i>Prunus laurocerasus</i>	3.676	11.445	12.916	10.977	9.754
Species	PM _{2.5-10} ($\mu\text{g cm}^{-2}$)				
	Spring	Summer	Fall	Winter	Annual Average
<i>Elaeagnus × ebbingei</i>	3.632	3.526	3.684	3.521	3.591
<i>Forsythia × intermedia</i>	2.81	2.964	2.587	-	2.787
<i>Laurus nobilis</i>	1.834	2.985	2.96	3.044	2.706
<i>Ligustrum vulgare</i>	2.833	4.307	4.629	4.583	4.088
<i>Pittosporum tobira</i>	2.641	3.68	3.607	4.248	3.544
<i>Prunus laurocerasus</i>	2.07	4.262	3.015	3.589	3.234
Species	PM _{0.2-2.5} ($\mu\text{g cm}^{-2}$)				
	Spring	Summer	Fall	Winter	Annual Average
<i>Elaeagnus × ebbingei</i>	0.84	0.538	1.171	1.039	0.897
<i>Forsythia × intermedia</i>	0.876	0.7	0.702	-	0.759
<i>Laurus nobilis</i>	0.555	0.341	0.42	0.846	0.541
<i>Ligustrum vulgare</i>	0.567	1.8	0.917	1.013	1.074
<i>Pittosporum tobira</i>	1.137	1.056	0.683	0.999	0.969
<i>Prunus laurocerasus</i>	0.804	1.135	0.955	0.894	0.947
Species	depPM ₁₀ ($\mu\text{g cm}^{-2} \text{day}^{-1}$)				
	Spring	Summer	Fall	Winter	Annual Average
<i>Elaeagnus × ebbingei</i>	4.893	1.362	0.310	0.641	1.802
<i>Forsythia × intermedia</i>	3.790	1.221	0.229	-	1.747
<i>Laurus nobilis</i>	2.811	1.076	0.193	0.550	1.157
<i>Ligustrum vulgare</i>	3.497	2.002	0.353	0.825	1.669
<i>Pittosporum tobira</i>	4.151	1.579	0.296	0.787	1.703
<i>Prunus laurocerasus</i>	3.130	1.799	0.275	0.664	1.467
Species	depPM _{2.5} ($\mu\text{g cm}^{-2} \text{day}^{-1}$)				
	Spring	Summer	Fall	Winter	Annual Average
<i>Elaeagnus × ebbingei</i>	0.934	0.184	0.075	0.142	0.334
<i>Forsythia × intermedia</i>	0.89	0.233	0.048	-	0.391
<i>Laurus nobilis</i>	0.65	0.105	0.014	0.113	0.22
<i>Ligustrum vulgare</i>	0.522	0.589	0.05	0.136	0.324
<i>Pittosporum tobira</i>	1.209	0.352	0.047	0.152	0.44
<i>Prunus laurocerasus</i>	0.859	0.378	0.067	0.132	0.359

Table A3. Cont.

(b)					
Species	PM ₁₀₋₁₀₀ (µg cm ⁻²)				
	Spring	Summer	Fall	Winter	Annual Average
<i>Deutzia scabra</i>	6.629	5.265	7.929	-	6.607
<i>Euonymus japonicus</i>	17.195	13.369	14.745	12.723	14.508
<i>Forsythia × intermedia</i>	6.865	4.503	8.121	-	6.497
<i>Pittosporum tobira</i>	12.332	10.118	10.913	11.752	11.279
<i>Prunus laurocerasus</i>	9.37	9.857	15.527	11.93	11.671
<i>Viburnum tinus</i>	13.205	11.147	15.39	13.798	13.385
Species	PM _{2.5-10} (µg cm ⁻²)				
	Spring	Summer	Fall	Winter	Annual Average
<i>Deutzia scabra</i>	3.585	2.556	3.662	-	3.268
<i>Euonymus japonicus</i>	5.5	3.469	4.787	5.235	4.748
<i>Forsythia × intermedia</i>	3.442	2.279	3.002	-	2.908
<i>Pittosporum tobira</i>	4.202	3.337	4.047	4.075	3.915
<i>Prunus laurocerasus</i>	3.401	3.011	4.568	4.315	3.824
<i>Viburnum tinus</i>	4.581	2.867	3.555	4.18	3.796
Species	PM _{0.2-2.5} (µg cm ⁻²)				
	Spring	Summer	Fall	Winter	Annual Average
<i>Deutzia scabra</i>	0.907	0.724	1.119	-	0.917
<i>Euonymus japonicus</i>	1.222	1.076	1.215	1.397	1.228
<i>Forsythia × intermedia</i>	1.32	0.958	1.071	-	1.116
<i>Pittosporum tobira</i>	1.287	1.043	1.293	0.521	1.036
<i>Prunus laurocerasus</i>	0.733	0.538	1.16	1.052	0.871
<i>Viburnum tinus</i>	1.15	0.823	1.182	0.878	1.008
Species	depPM ₁₀ (µg cm ⁻² day ⁻¹)				
	Spring	Summer	Fall	Winter	Annual Average
<i>Deutzia scabra</i>	3.47	0.753	0.637	-	1.62
<i>Euonymus japonicus</i>	5.091	1.033	0.812	2.652	2.397
<i>Forsythia × intermedia</i>	3.631	0.755	0.55	-	1.645
<i>Pittosporum tobira</i>	4.167	1.007	0.716	1.816	1.927
<i>Prunus laurocerasus</i>	3.37	0.802	0.784	2.273	1.807
<i>Viburnum tinus</i>	4.522	0.833	0.629	1.928	1.978
Species	depPM _{2.5} (µg cm ⁻² day ⁻¹)				
	Spring	Summer	Fall	Winter	Annual Average
<i>Deutzia scabra</i>	0.624	0.165	0.15	-	0.313
<i>Euonymus japonicus</i>	0.923	0.252	0.166	0.543	0.471
<i>Forsythia × intermedia</i>	1.028	0.231	0.144	-	0.468
<i>Pittosporum tobira</i>	0.996	0.243	0.175	0.223	0.409
<i>Prunus laurocerasus</i>	0.607	0.12	0.157	0.431	0.329
<i>Viburnum tinus</i>	0.858	0.188	0.157	0.343	0.386

Table A4. Seasonal and annual deposition ($depPM_{x.cpa}$; $g\ m^{-2}\ ground^{-1}\ day^{-1}$) expressed per unit of canopy cover for both fractions by the six shrub species in Lugano (a) and Bolzano (b).

(a)					
Species	$depPM_{10.cpa}$ ($g\ m^{-2}\ ground^{-1}\ day^{-1}$)				
	Spring	Summer	Fall	Winter	Annual Average
<i>Elaeagnus × ebbingei</i>	0.221	0.072	0.016	0.035	0.086
<i>Forsythia × intermedia</i>	0.131	0.047	0.008	-	0.062
<i>Laurus nobilis</i>	0.117	0.045	0.008	0.023	0.048
<i>Ligustrum vulgare</i>	0.115	0.066	0.01	0.026	0.054
<i>Pittosporum tobira</i>	0.178	0.073	0.014	0.037	0.076
<i>Prunus laurocerasus</i>	0.195	0.11	0.017	0.038	0.090
$depPM_{2.5.cpa}$ ($g\ m^{-2}\ ground^{-1}\ day^{-1}$)					
Species	Spring	Summer	Fall	Winter	Annual Average
<i>Elaeagnus × ebbingei</i>	0.041	0.009	0.004	0.007	0.015
<i>Forsythia × intermedia</i>	0.031	0.009	0.002	-	0.014
<i>Laurus nobilis</i>	0.024	0.004	0.000	0.005	0.008
<i>Ligustrum vulgare</i>	0.017	0.02	0.001	0.004	0.010
<i>Pittosporum tobira</i>	0.048	0.016	0.002	0.007	0.019
<i>Prunus laurocerasus</i>	0.055	0.023	0.004	0.007	0.022
(b)					
Species	$depPM_{10.cpa}$ ($g\ m^{-2}\ ground^{-1}\ day^{-1}$)				
	Spring	Summer	Fall	Winter	Annual Average
<i>Deutzia scabra</i>	0.109	0.027	0.022	-	0.052
<i>Euonymus japonicus</i>	0.164	0.033	0.027	0.083	0.077
<i>Forsythia × intermedia</i>	0.115	0.026	0.019	-	0.053
<i>Pittosporum tobira</i>	0.165	0.042	0.028	0.072	0.077
<i>Prunus laurocerasus</i>	0.142	0.036	0.037	0.109	0.081
<i>Viburnum tinus</i>	0.161	0.032	0.025	0.074	0.073
$depPM_{2.5.cpa}$ ($g\ m^{-2}\ ground^{-1}\ day^{-1}$)					
Species	Spring	Summer	Fall	Winter	Annual Average
<i>Deutzia scabra</i>	0.006	0.005	-	0.006	0.010
<i>Euonymus japonicus</i>	0.029	0.009	0.005	0.016	0.015
<i>Forsythia × intermedia</i>	0.031	0.008	0.005	-	0.015
<i>Pittosporum tobira</i>	0.039	0.01	0.007	0.008	0.016
<i>Prunus laurocerasus</i>	0.027	0.005	0.008	0.019	0.015
<i>Viburnum tinus</i>	0.033	0.007	0.006	0.013	0.015

References

- Jato-Espino, D.; Capra-Ribeiro, F.; Moscardó, V.; del Pino, L.E.B.; Mayor-Vitoria, F.; Gallardo, L.O.; Carracedo, P.; Dietrich, K. A systematic review on the ecosystem services provided by green infrastructure. *Urban For. Urban Green.* **2023**, *86*, 127998. [[CrossRef](#)]
- Rotzer, T.; Rahman, M.A.; Moser-Reischl, A.; Pauleit, S.; Pretzsch, H. Process based simulation of tree growth and ecosystem services of urban trees under present and future climate conditions. *Sci. Total Environ.* **2019**, *676*, 651–664. [[CrossRef](#)] [[PubMed](#)]
- Fares, S.; Conte, A.; Alivernini, A.; Chianucci, F.; Grotti, M.; Zappitelli, I.; Petrella, F.; Corona, P. Testing removal of carbon dioxide, ozone, and atmospheric particles by Urban Parks in Italy. *Environ. Sci. Technol.* **2020**, *54*, 14910–14922. [[CrossRef](#)]
- Fini, A.; Vigevani, I.; Corsini, D.; Wężyk, P.; Bajorek-Zydroń, K.; Failla, O.; Cagnolati, E.; Mielczarek, L.; Comin, S.; Gibin, M.; et al. CO₂-assimilation, sequestration, and storage by urban woody species growing in parks and along streets in two climatic zones. *Sci. Total Environ.* **2023**, *903*, 166198. [[CrossRef](#)]

5. Manzini, J.; Hoshika, Y.; Carrari, E.; Sicard, P.; Watanabe, M.; Tanaka, R.; Badea, O.; Nicese, F.P.; Ferrini, F.; Paoletti, E. FlorTree: A unifying modelling framework for estimating the species-specific pollution removal by individual trees and shrubs. *Urban For. Urban Green*. **2023**, *85*, 127967. [[CrossRef](#)]
6. Mori, J.; Fini, A.; Burchi, G.; Ferrini, F. Carbon uptake and air pollution mitigation of different Evergreen shrub species. *Arboric. Urban For*. **2016**, *42*, 329–345. [[CrossRef](#)]
7. Abhijith, K.V.; Kumar, P.; Gallagher, J.; McNabola, A.; Baldauf, R.; Pilla, F.; Broderick, B.; Di Sabatino, S.; Pulvirenti, B. Air pollution abatement performances of green infrastructure in open road and built-up street canyon environments—A review. *Atmos. Environ.* **2017**, *162*, 71–86. [[CrossRef](#)]
8. Romanello, M.; Walawender, M.; Hsu, S.-C.; Moskeland, A.; Palmeiro-Silva, Y.; Scamman, D.; Smallcombe, J.W.; Abdullah, S.; Ades, M.; Al-Maruf, A. The 2025 report of the Lancet Countdown on health and climate change: Climate change action offers a lifeline. *Lancet* **2025**, *406*, 2804–2857. [[CrossRef](#)]
9. Nowak, D.J.; Crane, D.E. Carbon storage and sequestration by urban trees in the USA. *Environ. Pollut.* **2002**, *116*, 381–389. [[CrossRef](#)]
10. Jo, H.-K.; McPherson, E.G. Carbon storage and flux in urban residential greenspace. *J. Environ. Manag.* **1995**, *45*, 109–133. [[CrossRef](#)]
11. Weissert, L.F.; Salmond, J.A.; Schwendenmann, L. Photosynthetic CO₂ uptake and carbon sequestration potential of deciduous and evergreen tree species in an urban environment. *Urban Ecosyst.* **2017**, *20*, 663–674. [[CrossRef](#)]
12. Luo, X.; Chen, J.M.; Liu, J.; Black, T.A.; Croft, H.; Staebler, R.; He, L.; Arain, M.A.; Chen, B.; Mo, G.; et al. Comparison of big-leaf, two-big-leaf, and two-leaf upscaling schemes for evapotranspiration estimation using coupled carbon-water modeling. *J. Geophys. Res. Biogeosciences* **2018**, *123*, 207–225. [[CrossRef](#)]
13. McPherson, E.G.; Xiao, J.O.; van Doorn, N.S.; Johnson, N.; Albers, S.; Peper, P.J. Shade factors for 149 taxa of in-leaf urban trees in the USA. *Urban For. Urban Green*. **2018**, *31*, 204–211. [[CrossRef](#)]
14. Stratoupulos, L.M.F.; Häberle, D.K.H.; Pauleit, S. Effect of native habitat on the cooling ability of six nursery-grown tree species and cultivars for future roadside plantings. *Urban For. Urban Green*. **2018**, *30*, 37–45. [[CrossRef](#)]
15. Rahman, M.A.; Moser, A.; Rötzer, T.; Pauleit, S. Comparing the transpirational and shading effects of two contrasting urban tree species. *Urban Ecosyst.* **2019**, *22*, 683–697. [[CrossRef](#)]
16. Kabisch, N.; Korn, H.; Stadler, J.; Bonn, A. *Nature-Based Solutions to Climate Change Adaptation in Urban Areas: Linkages Between Science, Policy and Practice*; Springer Nature: Berlin/Heidelberg, Germany, 2017; pp. 1–11. [[CrossRef](#)]
17. Rahman, M.A.; Stratopoulos, L.M.F.; Moser-Reischl, A.; Zolch, T.; Haberle, K.H.; Rotzer, T.; Pretzsch, H.; Pauleit, S. Traits of trees for cooling urban heat islands: A meta-analysis. *Build. Environ.* **2020**, *170*, 106606. [[CrossRef](#)]
18. Tiwary, A.; Reff, A.; Colls, J.J. Collection of ambient particulate matter by porous vegetation barriers: Sampling and characterization methods. *J. Aerosol Sci.* **2008**, *39*, 40–47. [[CrossRef](#)]
19. Mori, J.; Fini, A.; Galimberti, M.; Ginepro, M.; Burchi, G.; Massa, D.; Ferrini, F. Air pollution deposition on a roadside vegetation barrier in a Mediterranean environment: Combined effect of evergreen shrub species and planting density. *Sci. Total Environ.* **2018**, *643*, 725–737. [[CrossRef](#)]
20. Redondo-Bermúdez, M.; Gulenc, I.T.; Cameron, R.W.; Inkson, B.J. ‘Green barriers’ for air pollutant capture: Leaf micromorphology as a mechanism to explain plants capacity to capture particulate matter. *Environ. Pollut.* **2021**, *288*, 117809. [[CrossRef](#)]
21. Vigevani, I.; Corsini, D.; Comin, S.; Fini, A.; Ferrini, F. Methods to quantify particle air pollution removal by urban vegetation: A review. *Atmos. Environ. X* **2024**, *21*, 100233. [[CrossRef](#)]
22. Beloconi, A.; Vounatsou, P. Revised EU and WHO air quality thresholds: Where does Europe stand? *Atmos. Environ.* **2023**, *314*, 120110. [[CrossRef](#)]
23. Magarik, Y.A.; Roman, L.A.; Henning, J.G. How should we measure the DBH of multi-stemmed urban trees? *Urban For. Urban Green*. **2020**, *47*, 126481. [[CrossRef](#)]
24. De Mattos, E.M.; Binkley, D.; Campoe, O.C.; Alvares, C.A.; Stape, J.L. Variation in canopy structure, leaf area, light interception and light use efficiency among *Eucalyptus* clones. *For. Ecol. Manag.* **2020**, *463*, 118038. [[CrossRef](#)]
25. Leblanc, S.G.; Chen, J.M. A practical scheme for correcting multiple scattering effects on optical LAI measurements. *Agric. For. Meteorol.* **2001**, *110*, 125–139. [[CrossRef](#)]
26. White, M.A.; Asner, G.P.; Nemani, R.R.; Privette, J.L.; Running, S.W. Measuring fractional cover and leaf area index in arid ecosystems: Digital camera, radiation transmittance, and laser altimetry methods. *Remote Sens. Environ.* **2000**, *74*, 45–57. [[CrossRef](#)]
27. Sonnentag, O.; Talbot, J.; Chen, J.M.; Roulet, N.T. Using direct and indirect measurements of leaf area index to characterize the shrub canopy in an ombrotrophic peatland. *Agric. For. Meteorol.* **2007**, *144*, 200–212. [[CrossRef](#)]
28. Niu, X.; Fan, J.; Luo, R.; Fu, W.; Yuan, H.; Du, M. Continuous estimation of leaf area index and the woody-to-total area ratio of two deciduous shrub canopies using fisheye webcams in a semiarid loessial region of China. *Ecol. Indic.* **2021**, *125*, 107549. [[CrossRef](#)]

29. Beland, M.; Baldocchi, D.D. Vertical structure heterogeneity in broadleaf forests: Effects on light interception and canopy photosynthesis. *Agric. For. Meteorol.* **2021**, *307*, 108525. [[CrossRef](#)]
30. Comin, S.; Fini, A.; Napoli, M.; Frangi, P.; Vigevani, I.; Corsini, D.; Ferrini, F. Effects of severe pruning on the microclimate amelioration capacity and on the physiology of two urban tree species. *Urban For. Urban Green.* **2025**, *103*, 128583. [[CrossRef](#)]
31. Rana, G.; Ferrara, R.M.; Mazza, G. A model for estimating transpiration of rainfed urban trees in Mediterranean environment. *Theor. Appl. Climatol.* **2019**, *138*, 683–699. [[CrossRef](#)]
32. Vigevani, I.; Corsini, D.; Mori, J.; Pasquinelli, A.; Gibin, M.; Comin, S.; Szwajko, P.; Cagnolati, E.; Ferrini, F.; Fini, A. Particulate pollution capture by seventeen woody species growing in parks or along roads in two European cities. *Sustainability* **2022**, *14*, 1113. [[CrossRef](#)]
33. Song, S.; Leng, H.; Feng, S.; Meng, C.; Luo, B.; Zhao, L.; Zhang, C. Biomass allocation pattern of urban shrubs in the Yangtze River Delta region, China—a field observation of 13 shrub species. *Urban For. Urban Green.* **2021**, *63*, 127228. [[CrossRef](#)]
34. Tommila, T.; Tahvonen, O.; Kuittinen, M. How much carbon can shrubs store? Measurements and analyses from Finland. *Urban For. Urban Green.* **2024**, *101*, 128560. [[CrossRef](#)]
35. Pan, N.; Wang, S.; Wei, F.; Shen, M.; Fu, B. Inconsistent changes in NPP and LAI determined from the parabolic LAI versus NPP relationship. *Ecol. Indic.* **2021**, *131*, 108134. [[CrossRef](#)]
36. Nunes, L.; Pasalodos-Tato, M.; Alberdi, I.; Sequeira, A.C.; Vega, J.A.; Silva, V.; Vieira, P.; Rego, F.C. Bulk density of shrub types and tree crowns to use with forest inventories in the Iberian Peninsula. *Forests* **2022**, *13*, 555. [[CrossRef](#)]
37. Nelson, K.N.; Barnard, J.C.; Massingham, P.M.; Crotteau, J.S. Tree pruning improves tree form but not understory plant production in mixed stands of Sitka spruce and western hemlock, USA. *Forestry* **2024**, *97*, 309–318. [[CrossRef](#)]
38. Bequet, R.; Kint, V.; Campioli, M.; Vansteenkiste, D.; Muys, B.; Ceulemans, R. Influence of stand, site and meteorological variables on the maximum leaf area index of beech, oak and Scots pine. *Eur. J. For. Res.* **2012**, *131*, 283–295. [[CrossRef](#)]
39. Attarod, P.; Miri, S.; Shirvany, A.; Bayramzadeh, V. Variations in Leaf Area Index of *Quercus brantii* trees in response to changing climate. *J. Agric. Sci. Tech.* **2018**, *20*, 1417–1429. [[CrossRef](#)]
40. Fini, A.; Loreto, F.; Tattini, M.; Giordano, C.; Ferrini, F.; Brunetti, C.; Centritto, M. Mesophyll conductance plays a central role in leaf functioning of Oleaceae species exposed to contrasting sunlight irradiance. *Physiol. Plant.* **2016**, *157*, 54–68. [[CrossRef](#)] [[PubMed](#)]
41. Wang, J.; Zhou, Y.; Ji, C.; Xie, L.; Liu, Q.; Zhang, Z. Dynamic Simulation of the Leaf Mass per Area (LMA) in Multilayer Crowns of Young *Larix principis-rupprechtii*. *Plants* **2024**, *13*, 1223. [[CrossRef](#)]
42. Zhang, M.; Shen, J.; Wu, Y.; Zhang, X.; Zhao, Z.; Wang, J.; Cheng, T.; Zhang, Q.; Pan, H. Comparative transcriptome analysis identified *ChlH* and *POLGAMMA2* in regulating yellow-leaf coloration in *Forsythia*. *Front. Plant Sci.* **2022**, *13*, 1009575. [[CrossRef](#)]
43. Shi, Q.; He, B.; Knauer, J.; Peguero-Pina, J.J.; Zhang, S.B.; Huang, W. Leaf nutrient basis for the differentiation of photosynthetic traits between subtropical evergreen and deciduous trees. *Plant Physiol.* **2025**, *197*, kiae566. [[CrossRef](#)]
44. Moreno-Gutiérrez, C.; Dawson, T.E.; Nicolás, E.; Querejeta, J.I. Isotopes reveal contrasting water use strategies among coexisting plant species in a Mediterranean ecosystem. *New Phytol.* **2012**, *196*, 489–496. [[CrossRef](#)]
45. Korsakova, S.; Plugatar, Y.; Kovalev, M. Quantification of some ornamental plant species carbon dioxide absorption for various moisture conditions. In *E3S Web of Conferences*; EDP Sciences: Les Ulis, France, 2021; Volume 254, p. 06013. [[CrossRef](#)]
46. Toscano, S.; Scuderì, D.; Giuffrida, F.; Romano, D. Responses of Mediterranean ornamental shrubs to droughtstress and recovery. *Sci. Hortic.* **2014**, *178*, 145–153. [[CrossRef](#)]
47. Wang, J.; Shen, J.; Gu, M.; Wang, J.; Cheng, T.; Pan, H.; Zhang, Q. Leaf Coloration and Photosynthetic Characteristics of Hybrids between *Forsythia* ‘Courtaneur’ and *Forsythia koreana* ‘Suwon Gold’. *HortScience* **2017**, *52*, 1661–1667. [[CrossRef](#)]
48. Rossi, L.; Menconi, M.E.; Grohmann, D.; Brunori, A.; Nowak, D.J. Urban planning insights from tree inventories and their regulating ecosystem services assessment. *Sustainability* **2022**, *14*, 1684. [[CrossRef](#)]
49. Wiström, B.; Nielsen, A.B. Effects of planting design on planted seedlings and spontaneous vegetation 16 years after establishment of forest edges. *New For.* **2014**, *45*, 97–117. [[CrossRef](#)]
50. Edmondson, J.; Stott, I.; Davies, Z.; Gaston, K.; Leake, J. Soil surface temperatures reveal moderation of the urban heat island effect by trees and shrubs. *Sci. Rep.* **2016**, *6*, 33708. [[CrossRef](#)] [[PubMed](#)]
51. Zhang, R. Cooling effect and control factors of common shrubs on the urban heat island effect in a southern city in China. *Sci. Rep.* **2020**, *10*, 17317. [[CrossRef](#)]
52. Liu, X.; Li, X.-X.; Harshan, S.; Roth, M.; Velasco, E. Evaluation of an urban canopy model in a tropical city: The role of tree evapotranspiration. *Environ. Res. Lett.* **2017**, *12*, 094008. [[CrossRef](#)]
53. Vaigro-Wolff, A.L.; Warmund, M.R. Suppression of growth and plant moisture stress of *Forsythia* with flurprimidol and XE-1019. *HortScience* **1987**, *22*, 884–885. [[CrossRef](#)]
54. Schwaab, J.; Meier, R.; Mussetti, G.; Seneviratne, S.; Bürgi, C.; Davin, E.L. The role of urban trees in reducing land surface temperatures in European cities. *Nat. Commun.* **2021**, *12*, 6763. [[CrossRef](#)]

55. Konarska, J.; Uddling, J.; Holmer, B.; Lutz, M.; Lindberg, F.; Pleijel, H.; Thorsson, S. Transpiration of urban trees and its cooling effect in a high latitude city. *Int. J. Biometeorol.* **2016**, *60*, 159–172. [[CrossRef](#)]
56. Smith, I.A.; Winbourne, J.B.; Tieskens, K.F.; Jones, T.S.; Bromley, F.L.; Li, D.; Hutyra, L.R. A satellite-based model for estimating latent heat flux from urban vegetation. *Front. Ecol. Evol.* **2021**, *9*, 695995. [[CrossRef](#)]
57. Nowak, D.J.; Crane, D.E.; Stevens, J.C. Air pollution removal by urban trees and shrubs in the United States. *Urban For. Urban Green.* **2006**, *4*, 115–123. [[CrossRef](#)]
58. Beckett, K.P.; Freer-Smith, P.; Taylor, G. Effective tree species for local air-quality management. *J. Arboric.* **2000**, *26*, 12–19. [[CrossRef](#)]
59. Chen, L.; Liu, C.; Zhang, L.; Zou, R.; Zhang, Z. Variation in tree species ability to capture and retain airborne fine particulate matter (PM_{2.5}). *Sci. Rep.* **2017**, *7*, 3206. [[CrossRef](#)] [[PubMed](#)]
60. Weerakkody, U.; Dover, J.W.; Mitchell, P.; Reiling, K. Quantification of the traffic-generated particulate matter capture by plant species in a living wall and evaluation of the important leaf characteristics. *Sci. Total Environ.* **2018**, *635*, 1012–1024. [[CrossRef](#)]
61. Baraldi, R.; Chieco, C.; Neri, L.; Facini, O.; Rapparini, F.; Morrone, L.; Rotondi, A.; Carriero, G. An integrated study on air mitigation potential of urban vegetation: From a multi-trait approach to modeling. *Urban For. Urban Green.* **2019**, *41*, 127–138. [[CrossRef](#)]
62. Liu, L.; Guan, D.; Peart, M.R. The morphological structure of leaves and the dust-retaining capability of afforested plants in urban Guangzhou, South China. *Environ. Sci. Pollut. Res.* **2012**, *19*, 3440–3449. [[CrossRef](#)] [[PubMed](#)]
63. Mori, J.; Sæbø, A.; Hanslin, H.M.; Teani, A.; Ferrini, F.; Fini, A.; Burchi, G. Deposition of traffic-related air pollutants on leaves of six evergreen shrub species during a Mediterranean summer season. *Urban For. Urban Green.* **2015**, *14*, 264–273. [[CrossRef](#)]
64. Dzierzanowski, K.; Popek, R.; Gawronska, H.; Sæbø, A.; Gawronski, S.W. Deposition of particulate matter of different size fractions on leaf surfaces and in waxes of urban forest species. *Int. J. Phytoremediat.* **2011**, *13*, 1037–1046. [[CrossRef](#)]
65. Jouraeva, V.A.; Johnson, D.L.; Hassett, J.P.; Nowak, D.J. Differences in accumulation of PAHs and metals on the leaves of *Tilia × euchlora* and *Pyrus calleryana*. *Environ. Pollut.* **2002**, *120*, 331–338. [[CrossRef](#)]
66. Esposito, F.; Memoli, V.; Panico, S.C.; Di Natale, G.; Trifuoggi, M.; Giarra, A.; Maisto, G. Leaf traits of *Quercus ilex* L. affect particulate matter accumulation. *Urban For. Urban Green.* **2020**, *54*, 126780. [[CrossRef](#)]
67. Sæbø, A.; Popek, R.; Nawrot, B.; Hanslin, H.M.; Gawronska, H.; Gawronski, S.W. Plant species differences in particulate matter accumulation on leaf surfaces. *Sci. Total Environ.* **2012**, *427*, 347–354. [[CrossRef](#)]
68. Ottelé, M.; van Bohemen, H.D.; Fraaij, A.L. Quantifying the deposition of particulate matter on climber vegetation on living walls. *Ecol. Eng.* **2010**, *36*, 154–162. [[CrossRef](#)]
69. Hofman, J.; Stokkaer, I.; Snauwaert, L.; Samson, R. Spatial distribution assessment of particulate matter in an urban street canyon using biomagnetic leaf monitoring of tree crown deposited particles. *Environ. Pollut.* **2013**, *183*, 123–132. [[CrossRef](#)]
70. Baldauf, R. Roadside vegetation design characteristics can improve local, near-road air quality. *Transp. Res. Part D Transp. Environ.* **2017**, *52*, 354–361. [[CrossRef](#)] [[PubMed](#)]
71. Beckett, K.P.; Freer-Smith, P.H.; Taylor, G. Urban woodlands: Their role in reducing the effects of particulate pollution. *Environ. Pollut.* **1998**, *99*, 347–360. [[CrossRef](#)]
72. Janhäll, S. Review on urban vegetation and particle air pollution–deposition and dispersion. *Atmos. Environ.* **2015**, *105*, 130–137. [[CrossRef](#)]
73. Xie, C.; Kan, L.; Guo, J.; Jin, S.; Li, Z.; Chen, D.; Li, X.; Che, S. A dynamic processes study of PM retention by trees under different wind conditions. *Environ. Pollut.* **2018**, *233*, 315–322. [[CrossRef](#)]
74. Wang, H.; Shi, H.; Li, Y.; Yu, Y.; Zhang, J. Seasonal variations in leaf capturing of particulate matter, surface wettability and micromorphology in urban tree species. *Front. Environ. Sci. Eng.* **2013**, *7*, 579–588. [[CrossRef](#)]
75. Xu, X.; Xia, J.; Gao, Y.; Zheng, W. Additional focus on particulate matter wash-off events from leaves is required: A review of studies of urban plants used to reduce airborne particulate matter pollution. *Urban For. Urban Green.* **2020**, *48*, 126559. [[CrossRef](#)]
76. Prajapati, S.K.; Tripathi, B.D. Seasonal variation of leaf dust accumulation and pigment content in plant species exposed to urban particulates pollution. *J. Environ. Qual.* **2008**, *37*, 865–870. [[CrossRef](#)]
77. Bealey, W.J.; McDonald, A.G.; Nemitz, E.; Donovan, R.; Dragosits, U.; Duffy, T.R.; Fowler, D. Estimating the reduction of urban PM₁₀ concentrations by trees within an environmental information system for planners. *J. Environ. Manag.* **2007**, *85*, 44–58. [[CrossRef](#)] [[PubMed](#)]
78. Mitchell, R.; Maher, B.A.; Kinnersley, R. Rates of particulate pollution deposition onto leaf surfaces: Temporal and inter-species magnetic analyses. *Environ. Pollut.* **2010**, *158*, 1472–1478. [[CrossRef](#)] [[PubMed](#)]
79. Hewitt, C.N.; Ashworth, K.; MacKenzie, A.R. Using green infrastructure to improve urban air quality (GI4AQ). *Ambio* **2020**, *49*, 62–73. [[CrossRef](#)] [[PubMed](#)]
80. Przybysz, A.; Sæbø, A.; Hanslin, H.M.; Gawronski, S.W. Accumulation of particulate matter and trace elements on vegetation as affected by pollution level, rainfall and the passage of time. *Sci. Total Environ.* **2014**, *481*, 360–369. [[CrossRef](#)]

81. Pikridas, M.; Tasoglou, A.; Florou, K.; Pandis, S.N. Characterization of the origin of fine particulate matter in a medium size urban area in the Mediterranean. *Atmos. Environ.* **2013**, *80*, 264–274. [[CrossRef](#)]
82. Popek, R.; Haynes, A.; Przybysz, A.; Robinson, S.A. How much does weather matter? Effects of rain and wind on PM accumulation by four species of Australian native trees. *Atmosphere* **2019**, *10*, 633. [[CrossRef](#)]

Disclaimer/Publisher’s Note: The statements, opinions and data contained in all publications are solely those of the individual author(s) and contributor(s) and not of MDPI and/or the editor(s). MDPI and/or the editor(s) disclaim responsibility for any injury to people or property resulting from any ideas, methods, instructions or products referred to in the content.